Developmental Biology 453 (2019) 68–85

Contents lists available at ScienceDirect

Developmental Biology

journal homepage: www.elsevier.com/locate/developmentalbiology

Cortex glia clear dead young neurons via Drpr/dCed-6/Shark and Crk/Mbc/dCed-12 signaling pathways in the developing *Drosophila* optic lobe

Ryosuke Nakano [a,b], Masashi Iwamura [a], Akiko Obikawa [a,b], Yu Togane [a], Yusuke Hara [a], Toshiyuki Fukuhara [a], Masatoshi Tomaru [b], Toshiyuki Takano-Shimizu [b], Hidenobu Tsujimura [a,*]

[a] Tokyo University of Agriculture and Technology, 3-5-8 Saiwai-cho, Fuchu-shi, Tokyo 183-8509, Japan
[b] Department of Drosophila Genomics and Genetic Resources, Center for Advanced Insect Research Promotion, Kyoto Institute of Technology, Saga Ippongi-cho, Ukyo-ku, Kyoto 616-8354, Japan

ARTICLE INFO

Keywords:
Drosophila
Corpse clearance
Cortex glia
Drpr/dCed-6/Shark
Crk/Mbc/dCed-12
Optic lobe development

ABSTRACT

The molecular and cellular mechanism for clearance of dead neurons was explored in the developing *Drosophila* optic lobe. During development of the optic lobe, many neural cells die through apoptosis, and corpses are immediately removed in the early pupal stage. Most of the cells that die in the optic lobe are young neurons that have not extended neurites. In this study, we showed that clearance was carried out by cortex glia via a phagocytosis receptor, Draper (Drpr). *drpr* expression in cortex glia from the second instar larval to early pupal stages was required and sufficient for clearance. Drpr that was expressed in other subtypes of glia did not mediate clearance. Shark and Ced-6 mediated clearance of Drpr. The Crk/Mbc/dCed-12 pathway was partially involved in clearance, but the role was minor. Suppression of the function of Pretaporter, CaBP1 and phosphatidylserine delayed clearance, suggesting a possibility for these molecules to function as Drpr ligands in the developing optic lobe.

1. Introduction

In the vertebrate central nervous system (CNS), excess numbers of neurons are produced during development. Many of these superfluous cells die later, and the mature nervous system develops from neurons that have survived cell death. The clearance of dead neurons from the CNS is the last important step in completion of this cell death process.

Many studies have explored the cellular and molecular mechanisms for clearance of dead neurons in the developing *Drosophila* CNS (Kurant, 2011). During embryonic development, dead neurons are phagocytosed by subperineurial glia (Sonnenfeld and Jacobs, 1995). Draper (Drpr) acts as a phagocytosis receptor on the glial membrane to clear dead neurons in the embryo (Freeman et al., 2003). Another receptor, Six-microns-under (SIMU), works in cortex glia to allow recognition and engulfment of apoptotic cells, whereas Drpr works to degrade apoptotic cells in the embryonic CNS (Kurant et al., 2008). During metamorphosis, dead neurons are engulfed by glia in the CNS (Cantera and Technau, 1996). Elimination of neurites of vCrz neurons during metamorphosis is performed by astrocyte-like glia via the Crk/Mbc/dCed-12 signaling pathway but not the Drpr pathway (Tasdemir-Yilmaz and Freeman, 2014). In contrast, elimination of cell bodies of vCrz neurons requires Drpr, but its expression is not required in astrocyte-like glia (Tasdemir-Yilmaz and Freeman, 2014). However, recent studies have reported inconsistent results on the requirement of Drpr for dead cell clearance and the glia subtypes that work for clearance in the brain during metamorphosis. Etchegaray et al. (2016) reported that dead neurons that died in the central brain before the beginning of the third larval instar and in the optic lobe before the late third larval instar are cleared by cortex glia via the Drpr pathway, but neurons that die thereafter are efficiently cleared without Drpr. Hilu-Dadia et al. (2018) reported that Drpr is required for apoptotic cell clearance during metamorphosis and its expression is required in ensheathing glia and astrocyte-like glia, but not in cortex glia.

One of the causes of inconsistency among previous studies may be differences in the cellular materials to be phagocytosed, and different mechanisms could work for phagocytosis of different materials in the CNS during metamorphosis. Three types of neurons need to be phagocytosed during metamorphosis (Truman et al., 1993). Obsolete larval neurons die, and their cell bodies and neurites are removed by phagocytosis (Robinow et al., 1993; Nakano et al., 2001; Choi et al., 2006;

* Corresponding author. Laboratory of Student Science, Okuji 22, Kanegochi-cho, Ayabe-shi, Kyoto 623-0342, Japan.
E-mail address: tsujmr@cc.tuat.ac.jp (H. Tsujimura).

https://doi.org/10.1016/j.ydbio.2019.05.003
Received 22 August 2018; Received in revised form 25 April 2019; Accepted 2 May 2019
Available online 4 May 2019

Winbush and Weeks, 2011; Tasdemir-Yilmaz and Freeman, 2014). Larval neurons of another type are respecified from larval to adult neurons via pruning of larval neurites and extension of new adult neurites (Consoulas et al., 2002; Awasaki and Ito, 2004). Pruned neurites are removed by phagocytosis. Adult-specific neurons are produced by precursor cells during post-embryonic development and differentiate during metamorphosis (Truman et al., 1993; Meinertzhagen and Hanson, 1993). A number of these young neurons die during development before extending neurites (Fischbach and Technau, 1984; Togane et al., 2012; Jiang and Reichert, 2012; Hara et al., 2018). Therefore, studies on a single type of neuron or specifically defined neurons are needed to define the molecular and cellular mechanisms for clearance of dead neurons. Moreover, considering the report by Tasdemir-Yilmaz and Freeman (2014), clearance of neurites and cell bodies of dead neurons should be studied independently.

In this study, clearance of dead neurons in the developing optic lobe was examined. The *Drosophila* optic lobe is a unique center in which a large number of dying cells are observed during its development (Fischbach and Technau, 1984; Togane et al., 2012). Most dying neurons in the optic lobe are young neurons that had just started to differentiate into adult neurons. One of paired neurons derived from intermediate precursors (GMCs) is eliminated by apoptosis under the control of Notch signaling (Bertet et al., 2014; Erclik et al., 2017). Neurons that die in the developing optic lobe have not yet extended neurites at the time they die (Hara et al., 2018). Therefore, cellular materials to be cleared after the cell death include nuclei and general cytoplasm, but not neurites in the developing optic lobe.

The adult optic lobe develops from the primordium during metamorphosis. Optic lobe neurons are produced by two proliferation centers, the outer proliferation center (OPC) and inner proliferation center (IPC) (Meinertzhagen and Hanson, 1993; Fischbach and Hiesinger, 2008; Sato et al., 2013). Neurons differentiate, extend neurites, and produce four types of neuropil, the lamina, medulla, lobula plate, and lobula. Then, the optic lobe consists of four types of neuropil and surrounding cortices of neuronal cell bodies. According to previous studies, many neurons and a small number of precursor cells undergo cell death during optic lobe development (Togane et al., 2012; Akagawa et al., 2015; Hara et al., 2018). This cell death does not occur randomly in the optic lobe but occurs in clusters in a specific temporal and spatial pattern (Togane et al., 2012; Akagawa et al., 2015). The number of dead cells in the optic lobe starts to increase at the puparium formation, reaches a peak at 24 h after puparium formation (24 h APF), and decreases to almost zero by 48 h APF. Two types of cell death are involved in this process: ecdysone dependent and independent (Hara et al., 2013). Both types of cell death are apoptosis and involve the *Drosophila* effector caspases, DrIce and Dcp-1 (Akagawa et al., 2015). DrIce plays an important role in dead cell clearance as well (Akagawa et al., 2015). The role of cell death is to prevent the emergence of abnormal neural structures in the optic lobe (Hara et al., 2018).

In this study, we explored the cellular and molecular mechanisms for clearance of dead young neurons in the developing optic lobe. The results showed that clearance was carried out by cortex glia via a phagocytosis receptor, Drpr. Drpr expression in cortex glia from the second instar larval to early pupal stages was required and sufficient for clearance. Signaling molecules, Shark and Ced-6 mediated clearance downstream of Drpr. The Crk/Mbc/dCed-12 pathway was partially involved in clearance, but the role was minor. Suppression of the function of Pretaporter, CaBP1 and phosphatidylserine delayed clearance, suggesting a possibility for these molecules to function as Drpr ligands in the developing optic lobe.

2. Results

2.1. Drpr is required for clearance of dead young neurons in the developing optic lobe

The number of dead neurons starts to increase at the beginning of metamorphosis in the developing optic lobe in wild-type flies, reaches a peak at 24 h APF, and decreases thereafter to almost none by 48 h (Fig. 1A and B, present study; Togane et al., 2012; Akagawa et al., 2015). This suggests that dead neuronal cells are actively removed from the optic lobe between 0 and 48 h APF. Here we first examined the function of Drpr in clearance of dead neurons in the developing optic lobe. Drpr functions in the clearance of dead neurons in the CNS in the embryonic stage and during metamorphosis (Freeman et al., 2003; Kurant et al., 2008; Tasdemir-Yilmaz and Freeman, 2014; Etchegaray et al., 2016; Hilu-Dadia et al., 2018). However, Etchegaray et al. (2016) reported that dead neurons that died after the beginning of the third larval instar in the central brain and after the late third larval instar in the optic lobe are efficiently cleared without Drpr. In addition, Hilu-Dadia et al. (2018), who reported that Drpr is required for apoptotic cell clearance during metamorphosis, mentioned nothing about the clearance of dead neurons that died after 24 h APF.

We investigated the alteration in the number of terminal deoxynucleotidyl transferase dUTP nick end labeling (TUNEL)-positive cells in the developing optic lobe in *drpr* mutants ($drpr^{\Delta 5}$). The results showed that a much greater number of TUNEL-positive cells was observed in *drpr* mutants than in the wild type (Fig. 1A). In *drpr* mutants, from the anterior view, TUNEL-positive signals overlapped in the peripheral region of the optic lobe, and we could not count the exact number of TUNEL-positive cells in the optic lobe. Therefore, we described the number of TUNEL-positive cells in those samples as “uncountable” in this study (Fig. 1A and B). An uncountable number of TUNEL-positive cells was continuously observed from the early pupal stage (0 h APF) to the adult stage (120 h APF). Of particular interest, an enormous number of TUNEL-positive cells was observed even 1 day after eclosion without signs of decline, whereas dead cells were rarely seen in the wild type. We hypothesized that this uncountable number of TUNEL-positive dead cells accumulated due to the defect in dead cell clearance caused by the *drpr* mutation. To test this idea, we examined phagocytic activity using Lysotracker staining in *drpr* mutant optic lobes. In wild-type optic lobes, Lysotracker signals appeared at a location that was consistent with dead cells (Fig. 1C, present study; Akagawa et al., 2015). In *drpr* mutants, Lysotracker signals were significantly decreased (Fig. 1D) and nearly absent throughout the entire optic lobe (Fig. 1C). Therefore, we confirmed that drpr mutation inhibited dead cell clearance, resulting in abnormal accumulation of TUNEL-positive cells. This shows that drpr is necessary for clearance of dead neurons in the developing optic lobe.

Moreover, abnormal accumulation of TUNEL-positive cells in *drpr* mutants occurred across the entire optic lobe cortex (Fig. 1A, E). Most parts of the optic lobe develop after puparium formation, and development proceeds from medial to lateral in the medulla region and lateral to medial in the lamina region in early stages of metamorphosis (Sato et al., 2013; Hara et al., 2013). Dying cells were observed in clusters in the developing optic lobe in the wild type (Fig. 1E, present study; Togane et al., 2012; Akagawa et al., 2015). From single image sections from the dorsal view of developing *drpr* mutant optic lobes at 24 h and 48 h APF, we observed that TUNEL-positive cells had accumulated in the entire cortex of developing optic lobes, including regions of dying cell clusters that arose from 0 h to 48 h APF (Fig. 1E). Therefore, the necessity of *drpr* for clearance is general in the optic lobe, and is not limited to specific developmental stages or specific areas in the optic lobe.

2.2. drpr expression from late larval to early pupal stages is required to clear dead young neurons in the developing optic lobe

The above results are inconsistent with results from a previous study. Etchegaray et al. (2016) reported that in the optic lobe, Drpr is required for removal of dead neurons that died before the late third larval instar, but dying neurons that arose thereafter are efficiently cleared without Drpr. Thus, we performed the next experiment to confirm our previous result. We examined the period of *drpr* expression that is required for dead cell clearance in the optic lobe during development.

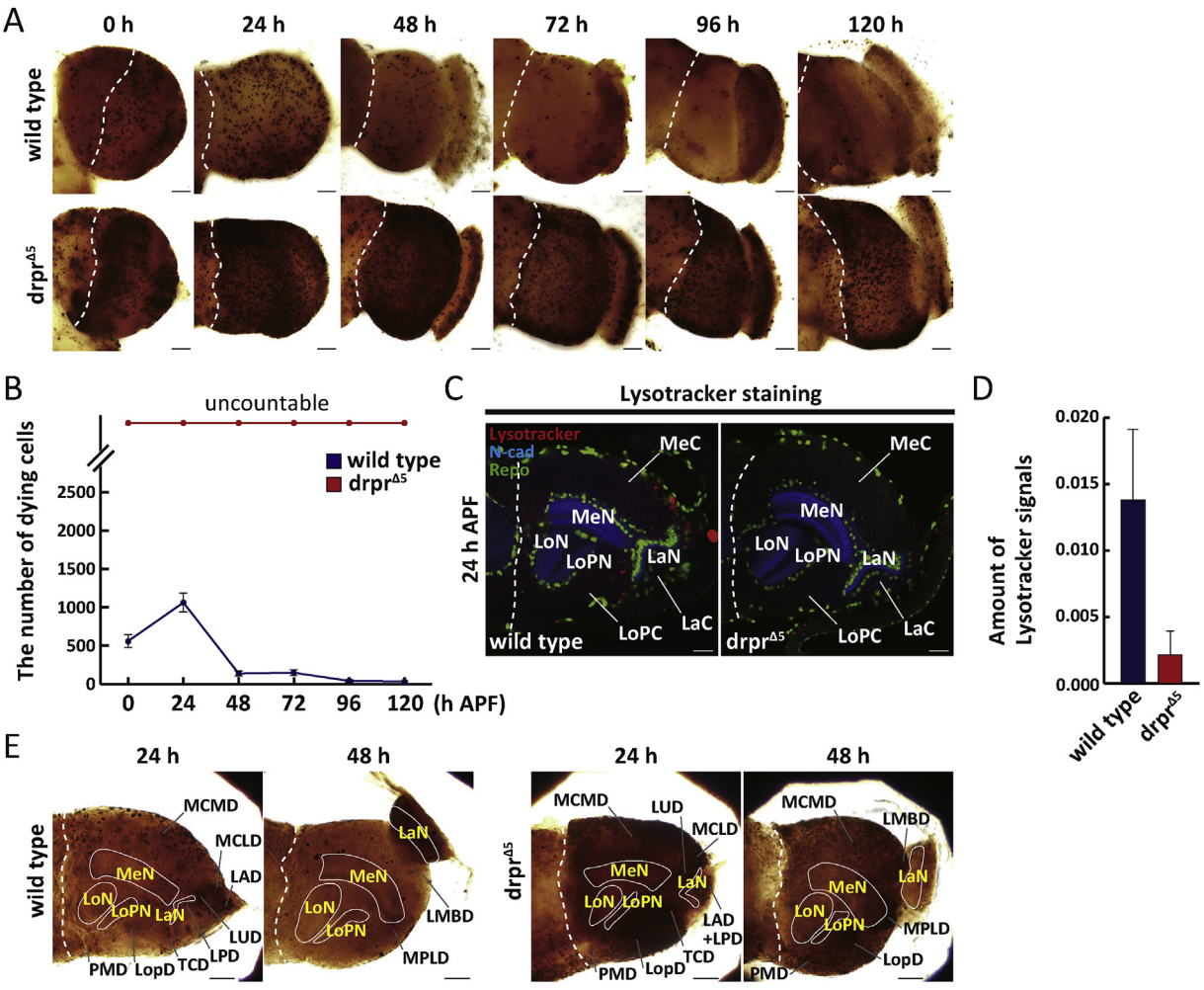

Fig. 1. *Draper* is required for dead cell clearance in the developing optic lobe. (A) TUNEL-positive cells in the developing optic lobe in $drpr^{\Delta 5}/drpr^{\Delta 5}$ and the wild type (Canton-S). Minimal projection of serial optical sections from the anterior view. (B) Temporal change in the number of dying cells in the optic lobe during metamorphosis in $drpr^{\Delta 5}/drpr^{\Delta 5}$ and the wild type. Mean ± SD. n = 10. (C) Lysosomal activity in the optic lobe in $drpr^{\Delta 5}/drpr^{\Delta 5}$ and the wild type. Dorsal view. Red: Lysotracker signal, Blue: anti-N-cadherin, Green: anti-Repo. LaC: lamina cortex, MeC: medulla cortex, LoPC: lobula plate cortex, LaN: lamina neuropil, MeN: medulla neuropil, LoN: lobula neuropil, LoPN: lobula plate neuropil. (D) Quantification of Lysotracker signals in the optic lobe in $drpr^{\Delta 5}/drpr^{\Delta 5}$ and the wild type. The number of Lysotracker-positive pixels (pixels) and optic-lobe-area (pixels) were counted from an optic section at the level of MCLD and Lysotracker-positive signals/optic-lobe area was calculated. Mean ± SD. n = 12 in $drpr^{\Delta 5}/drpr^{\Delta 5}$ and the wild type. $P < 0.05$ (Mann-Whitney test). (E) TUNEL-positive cells in the optic lobe in $drpr^{\Delta 5}/drpr^{\Delta 5}$ and the wild type. An optical section from the dorsal view. TUNEL-positive cells accumulated in $drpr^{\Delta 5}/drpr^{\Delta 5}$ in the entire cortex of developing optic lobes, including regions of dying cell clusters that arose from 0 h to 48 h APF. MCMD, MCLD, LAD, LUD, LPD, TCD, LopD, PMD, LMBD, and MPLD: dying cell clusters (Akagawa et al., 2015). In the wild type, MCMD arose at 12–36 h APF, MCLD at 12–24 h APF, LAD at 0–24 h, LUD at 24 h APF, LPD at 12–24 h APF, TCD at 0–24 h APF, LopD at 24–36 h APF, PMD at 0–36 h APF, LMBD at 36–48 h APF, and MPLD at 36–48 h APF (Akagawa et al., 2015). White dashed line: boundary between the optic lobe and the central brain.

hs-GAL4/UAS-*draper*-RNAi (*hs* > *drpr*-RNAi) insects were heat shocked at different developmental stages to induce temporary knockdown of *drpr*, and the number of TUNEL-positive cells accumulating in the optic lobe was analyzed (Fig. 2A, B, C).

When late third instar larvae (L3) were heat shocked for 30-min at 12–16 h before puparium formation and the insects were allowed to develop for up to 24 or 48 h APF (Fig. 2C, *hs* > *drpr*-RNAi hs L3), the number of TUNEL-positive cells in the optic lobe significantly increased by about 70% at 24 h APF and 320% at 48 h compared to negative controls and the wild type at the same stage (Fig. 2C, wild type hs -). Similar results were observed with pupae treated with a 1-h heat shock at 0 h APF (Fig. 2C, *hs* > *drpr*-RNAi hs 0 h APF). However, heat shock after 12 h APF (Fig. 2C, *hs* > *drpr*-RNAi hs 12 h APF) did not induce a significant increase in the number of TUNEL-positive cells compared to negative controls and the wild type (Fig. 2C, *hs* > *drpr*-RNAi hs-, wild type hs -). Therefore, *drpr* expression from late L3 to 12 h APF is necessary for dead cell clearance in the developing optic lobe, and expression after 12 h APF is dispensable.

Next, we investigated whether dead cell clearance was rescued with forced expression of wild-type *drpr* (*drpr1*) on the *drpr* mutant background (Fig. 2D, E, F). Heat shock was applied to *hs-GAL4*/UAS-*draper1*; $drpr^{\Delta 5}/drpr^{\Delta 5}$ (*hs* > *drpr1*; $drpr^{\Delta 5}$) at various developmental stages. Without heat shock, a large number of TUNEL-positive cells accumulated throughout the entire optic lobe at all stages (Fig. 2D, F). However, when a 30-min heat shock was applied to L3 and the larvae were allowed to develop for up to 0 h APF, and when a 1-h heat shock was given at 0 h APF and the pupae were allowed to develop for up to 24 and 48 h APF, the number of TUNEL-positive cells decreased to the same level as the wild type (Fig. 2D, F). Therefore, forced temporary expression of *drpr1* at stages from L3 to early pupa is sufficient for dead cell clearance in *drpr* mutants.

Moreover, forced expression of *drpr1* for 1-h at 24–72 h APF stages on the *drpr* mutant background decreased the number of TUNEL-positive cells to the same level as in the wild type (Fig. 2E and F). This shows

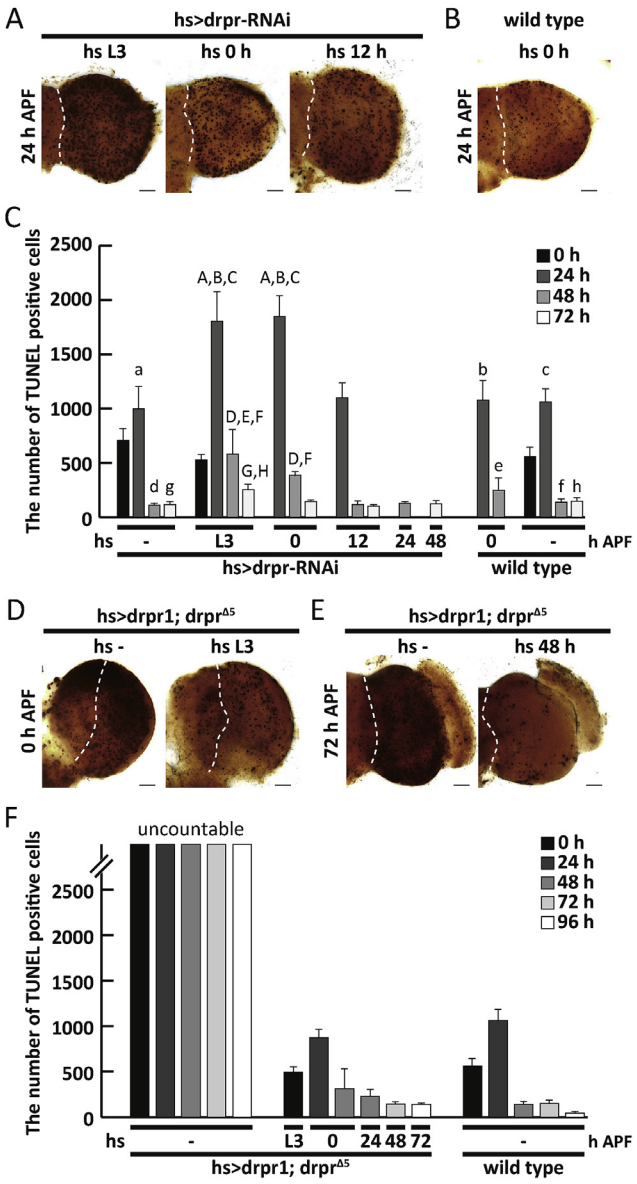

Fig. 2. *Drpr* expression at late larval and early pupal stages is required for dead cell clearance. (A) TUNEL-positive cells in optic lobes in *hs-GAL4/UAS-draper*-RNAi. Heat shock was applied for 30-min at late third larval instar (L3), 1-h at 0 h APF, and 1-h at 12 h APF. (B) TUNEL-positive cells in the wild-type optic lobe. Heat shock was applied for 1-h at 0 h APF. (C) The number of TUNEL-positive cells in optic lobes in *hs-GAL4/UAS-draper*-RNAi and in the wild type. Heat shock was applied for 30-min at late L3 and 1-h at 0, 12, 24, 48 h APF. A, D, G, B, C, E, F and H in heat-shocked *hs-GAL4/UAS-draper*-RNAi are significantly different from a, d, and g in non-heat-shocked *hs-GAL4/UAS-draper*-RNAi and b, c, e, f, and h in the wild type, respectively. Mean ± SD. n = 10 in the wild type and n = 5 in *hs-GAL4/UAS-draper*-RNAi. $P < 0.05$ (Kruskal-Wallis rank sum test and post hoc Wilcoxon rank sum test with Bonferroni correction). (D) TUNEL-positive cells in optic lobes in *hs-GAL4/UAS-draper1*; $drpr^{\Delta5}/drpr^{\Delta5}$. Heat shock was applied for 30-min at late L3. (E) TUNEL-positive cells in optic lobes in *hs-GAL4/UAS-draper1*; $drpr^{\Delta5}/drpr^{\Delta5}$. Heat shock was applied for 1-h at 48 h APF. (F) The number of TUNEL-positive cells in optic lobes in *hs-GAL4/UAS-draper1*; $drpr^{\Delta5}/drpr^{\Delta5}$ and in the wild type. Heat shock was applied for 30-min at late L3 and 1-h at 0, 24, 48, and 72 h APF. The number of TUNEL-positive cells was uncountable in non-heat-shocked *hs-GAL4/UAS-draper1*; $drpr^{\Delta5}/drpr^{\Delta5}$. No significant difference was found between heat-shocked *hs-GAL4/UAS-draper1*; $drpr^{\Delta5}/drpr^{\Delta5}$ and the wild type. Mean ± SD. n = 10 in the wild type and n = 5 in *hs-GAL4/UAS-draper1*; $drpr^{\Delta5}/drpr^{\Delta5}$. $P < 0.05$ (Kruskal-Wallis rank sum test and post hoc Wilcoxon rank sum test with Bonferroni correction).

that TUNEL-positive cells that accumulated in *drpr* mutants were sufficiently removed by forced temporary expression of *drpr1*, even at mid- and late pupal stages.

Altogether, these experiments supported the idea described in the previous section. Drpr expression from late larval to early pupal stages is required and sufficient to clear cell bodies of dead neurons in the developing optic lobe. Moreover, cellular function for corpse clearance is not limited to larval and early pupal stages in the developing optic lobe, but is active throughout all pupal stages when Drpr is forcibly expressed.

2.3. Drpr expressed in glia functions to clear dead young neurons in the developing optic lobe

Drpr expression in the CNS during metamorphosis was described in the ventral nerve cord (Tasdemir-Yilmaz and Freeman, 2014) and whole brain (Hilu-Dadia et al., 2018). However, no detailed description in the developing optic lobe has been published. Thus, we analyzed the alteration in the pattern of Drpr expression in the developing optic lobe with anti-Drpr antibody.

In the lamina region, Drpr was weakly expressed in the surface layer of the lamina region and the cortex at 0 h APF (Fig. 3A). The expression weakened by 24 h APF, but increased thereafter to be moderate again at 48 and 72 h APF. Drpr expression was moderate in the lamina neuropil from 0 h to 24 h APF and strong all over the lamina neuropil after 48 h APF (Fig. 3A, yellow arrowheads).

In the medulla, lobula plate, and lobula region (MLpL region), Drpr was moderately expressed in neuronal precursor cells in the OPC, and weakly in the IPC at 0 h APF (Fig. 3A). In the surface layer, Drpr expression was moderate at 0 h APF, weaker at 24 h APF, and remained weak at 72 h APF. In the cortex, Drpr was weakly expressed in a mesh-like pattern (Fig. 3A, white arrowheads), filling gaps among neural cells, and moderately expressed in a centripetal pattern of lines (Fig. 3A, white arrows) projecting from the outer side of the cortex to the neuropil surface at 0 h APF. The expression remained weak in a mesh-like pattern up to 72 h APF. The expression in a centripetal pattern of lines became stronger towards 24 h APF but weakened thereafter and disappeared by 48 h APF. On the medulla neuropil surface, Drpr expression was moderate at 0 h APF, rapidly increased to be strong at 12 h APF, and continued to 72 h APF (Fig. 3A, yellow asterisks). At 72 h APF, Drpr was also strongly expressed in many fine protrusions of glia (Fig. 3A 72 h, 72 h-2, yellow arrow) invading the distal medulla from the neuropil surface. Drpr was also expressed in fine protrusions of glia invading the proximal medulla, lobula plate and lobula neuropil from the MLpL neuropil surface (Fig. 3A 72 h, 72 h-2). Moderate Drpr staining was observed in the MLpL neuropil from 0 to 12 h APF (Fig. 3A, black asterisk) but became weak thereafter.

In the outer and inner chiasm (Fig. 3A), Drpr was weakly expressed throughout the entire pupal period.

The Drpr expression pattern in the optic lobe overlapped well with the glial processes visualized by repo > mCD8-GFP in the optic lobe surface, cortex, neuropil surface, and chiasm at all developmental stages except in neuronal precursor cells in the OPC and IPC, and the lamina and MLpL neuropils at early pupal periods (Fig. 3A). This suggests the possibility that Drpr is located on the glial cell membrane in the optic lobe surface, cortex, neuropil surface, and chiasm. However, the pattern also overlapped in the cortex with anti-N-cadherin staining, which detects neuronal cell membranes. Then, to determine the cell types that expressed Drpr, we performed cell type-specific *drpr* knockdown and examined Drpr expression (Fig. 3B).

When *drpr* was knocked down with a pan glial driver, *repo-GAL4*, which drives gene expression in all glial cells at all stages except in a small fraction of glial cells in early pupae (Fig. 5A, present study; Togane et al., 2012), Drpr staining was strongly decreased in all regions except the OPC and IPC at 0 h APF and the lamina and MLpL neuropils at 24 h APF (Fig. 3B). Moreover, spotted weak staining was observed in the medulla cortex at 24 h APF (Fig. 3B). In contrast, when we knocked down

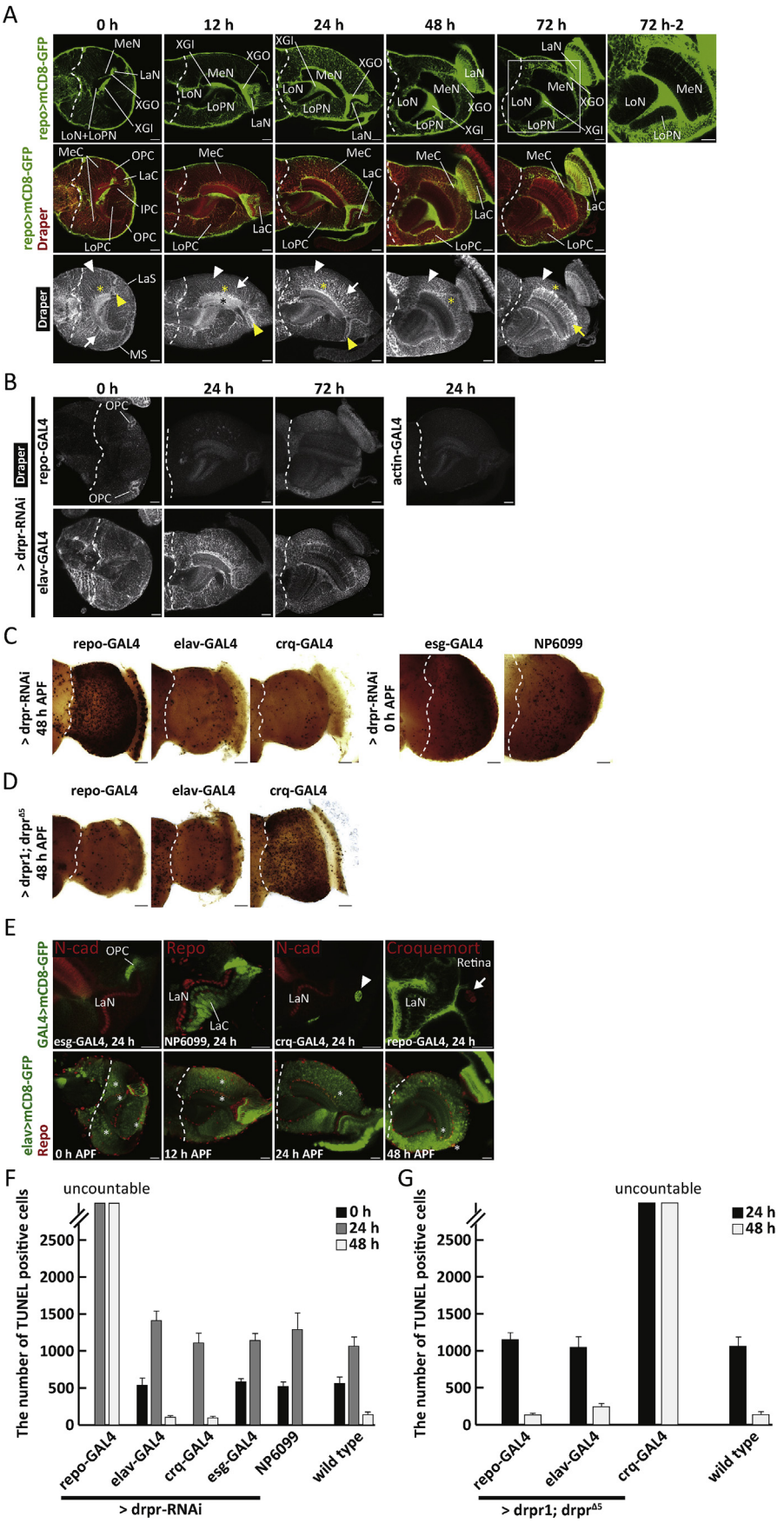

Fig. 3. Drpr expression in glia is required for dead cell clearance. (A) Draper expression in the developing optic lobe in *UAS-mCD8::GFP/+*; *repo-GAL4/+*. Green: *repo > mCD8-GFP*. Red and White: anti-Draper. White arrowhead: mesh-like pattern in the cortex. White arrow: centripetal pattern in the cortex. Yellow arrowhead: lamina neuropil. Yellow asterisks: the medulla neuropil surface. Black asterisk: MLpL neuropil. Yellow arrow: fine protrusion of glia into the neuropil. (B) Drpr expression in optic lobes in *UAS-draper*-RNAi/+; *repo-GAL4/+*, *elav-GAL4/+* or Y; *UAS-draper*-RNAi/+, *actin-GAL4/UAS-draper*-RNAi. White: anti-Drpr. (C) TUNEL-positive cells in optic lobes in *UAS-draper*-RNAi/+; *repo-GAL4/+*, *elav-GAL4/+* or Y; *UAS-draper*-RNAi/+, *crq-GAL4/UAS-draper*-RNAi, *esg-GAL4/UAS-draper*-RNAi, and *NP6099/+* or Y; *UAS-draper*-RNAi/+. (D) TUNEL-positive cells in optic lobes in *UAS-drpr1/+*; *repo-GAL4 drpr$^{\Delta5}$/drpr$^{\Delta5}$*, *elav-GAL4/+* or Y; *UAS-drpr1/+*; *drpr$^{\Delta5}$/drpr$^{\Delta5}$*, *crq-GAL4/UAS-drpr1*; *drpr$^{\Delta5}$/drpr$^{\Delta5}$*. (E) The expression pattern in tissue-specific GAL4s. *esg-GAL4/UAS-mCD8::GFP*, *NP6099/+* or Y; *UAS-mCD8::GFP/+*, *crq-GAL4/UAS-mCD8::GFP*, *UAS-mCD8::GFP/+*; *repo-GAL4/+*, *elav-GAL4/+* or Y; *UAS-mCD8::GFP/+*. Green: mCD8-GFP, Red: anti-N-cad, anti-Repo, or anti-Croquemort. Arrow and arrowhead: hemocytes outside the lamina cortex. Asterisks: glia that express *elav>mCD8-GFP*. (F) The number of TUNEL-positive cells in optic lobes in *UAS-draper*-RNAi/+; *repo-GAL4/+*, *elav-GAL4/+* or Y; *UAS-draper*-RNAi/+, *crq-GAL4/UAS-draper*-RNAi, *esg-GAL4/UAS-draper*-RNAi, and *NP6099/+* or Y; *UAS-draper*-RNAi/+. The number of TUNEL-positive cells in *UAS-draper*-RNAi/+; *repo-GAL4/+* was uncountable. No significant difference was found between the other *GAL4s > draper*-RNAi and the wild type. Mean ± SD. n = 10 in the wild type and n = 5 in the *GAL4s > draper*-RNAi. $P < 0.05$ (Kruskal-Wallis rank sum test and post hoc Wilcoxon rank sum test with Bonferroni correction). (G) The number of TUNEL-positive cells in optic lobes in *UAS-drpr1/+*; *repo-GAL4 drpr$^{\Delta5}$/drpr$^{\Delta5}$*, *elav-GAL4/+* or Y; *UAS-drpr1/+*; *drpr$^{\Delta5}$/drpr$^{\Delta5}$*, *crq-GAL4/UAS-drpr1*; *drpr$^{\Delta5}$/drpr$^{\Delta5}$*. The number of TUNEL-positive cells in *crq-GAL4/UAS-drpr1*; *drpr$^{\Delta5}$/drpr$^{\Delta5}$* was uncountable. No significant difference was found between the other *GAL4s > draper1*; *drpr$^{\Delta5}$/drpr$^{\Delta5}$* and the wild type. Mean ± SD. n = 10 in the wild type and n = 5 in the *GAL4s > draper1*; *drpr$^{\Delta5}$/drpr$^{\Delta5}$*. $P < 0.05$ (Kruskal-Wallis rank sum test and post hoc Wilcoxon rank sum test with Bonferroni correction).

drpr using the pan neural driver, *elav-GAL4*, which drives gene expression in all neural cells at all stages, the OPC and IPC, and a small fraction of glial cells in early pupae (Fig. 3E, present study; Togane et al., 2012; Hara et al., 2018), Drpr expression was observed in almost the same pattern as in the control at 0, 24, and 72 h APF (Fig. 3B). However, the expression was weaker in the OPC and IPC and the lamina and MLpL neuropils at 0 h APF. Moreover, when *drpr* was knocked down in all types of cells with *actin-GAL4*, Drpr expression almost completely disappeared at 24 h APF, and no spotted expression was observed in the medulla cortex, although weak staining remained in the lamina and MLpL neuropils, and lamina cortex (Fig. 3B).

Altogether, these results suggest that Drpr is mainly expressed in glial cells and the expression pattern of Drpr in the cortex agreed with the alteration in the activity of dead cell clearance during metamorphosis. At early pupal stages, Drpr is expressed weakly in a mesh-like pattern and strongly in a centripetal pattern in the cortex glia. This expression weakened thereafter, and only weak expression was seen in a mesh-like pattern during the last half of the pupal period. However, Drpr was also expressed in glia in the optic lobe surface, neuropil surface and chiasm at all developmental stages, neuronal precursor cells in the OPC and IPC at 0 h APF, and some spotted structures in the medulla cortex at 24 h APF. As weak staining remained in the lamina and MLpL neuropils and lamina cortex when *drpr* was knocked down with *actin-GAL4*, staining in the lamina and MLpL neuropils and some staining in the lamina cortex at early pupal stages may be non-specific staining, although control staining with only secondary antibody but no anti-Drpr antibody did not stain these structures.

Next, to examine the role of *drpr* expression in each type of cell, we performed *drpr* knockdown using cell type-specific GAL4 lines and examined the influence on dead cell clearance. The expression pattern of GAL4s is shown in Figs. 3E and 5A. The results showed that a large number of TUNEL-positive cells accumulated in pupae in which *drpr* knockdown was performed with *repo-GAL4* (Fig. 3C, F). The density and distribution of accumulated TUNEL-positive cells were the same as in *drpr* mutants. In contrast, we observed no significant increase when we used *elav-GAL4*, the hemocyte-specific driver *crq-GAL4*, the precursor cell (neuroblasts and neuroepithelial cells)-specific driver *esg-GAL4* (Hara et al., 2018), or the lamina neuronal cell-specific driver NP6099. Therefore, Drpr expression only in glial cells is necessary for the clearance of cell bodies of dead neurons in the developing optic lobe. We confirmed that hemocytes were unnecessary for clearance, because no hemocytes were present in the developing optic lobe (Fig. 3E).

Next, we performed rescue experiments. Forced expression of *drpr1* using cell-type specific GAL4s on the *drpr* mutant background showed that dead cell clearance was rescued with *repo-GAL4* (Fig. 3D, G). The number of dead cells in *repo > drpr1;drpr*$^{\triangle 5}$ was similar to that in the wild type. Therefore, *drpr* expression in glia is sufficient for dead cell clearance. Moreover, when we used *elav-GAL4* (in *elav-GAL4>drpr1*; *drpr*$^{\Delta 5}$), we found that the clearance was rescued to the same extent as in the wild type, both at 24 and 48 h APF (Fig. 3D, G). However, this fact does not mean that neurons can also clear dead cells when *drpr* is forcibly expressed. In *elav-GAL4*, in addition to expression in neurons, GAL4 is also expressed in a small fraction of glia in a lateral region of the medulla cortex and the medulla neuropil surface during 0–48 h APF and is never observed later (Fig. 3E, present study; Togane et al., 2012; Hara et al., 2018). These glial cells are young glia, as development proceeds from medial to lateral in the medulla cortex and medulla neuropil (Sato et al., 2013; Hara et al., 2013). Therefore, in *elav-GAL4*, glial cells in the medulla cortex and in the medulla neuropil surface transiently express GAL4 during an early phase of their development at early pupal stages. Therefore, in *elav-GAL4>drpr1*; *drpr*$^{\Delta 5}$, Drpr would have been transiently expressed in young glia in the medulla cortex and in the medulla neuropil surface, and these glia with Drpr would have cleared dead cells. No rescue was observed with *crq-GAL4* or NP6099, confirming that *drpr* expression in hemocytes or developing lamina neurons does not mediate clearance in the developing optic lobe.

Altogether, Drpr expression in glia is required and sufficient for clearing cell bodies of dead neurons during metamorphosis. This result agrees with the previous study (Hilu-Dadia et al., 2018).

2.4. Expression pattern of GAL4 in glial subtype-specific GAL4 lines in the developing optic lobe

From the above results, we concluded that Drpr expressed in glia mediates dead cell clearance in the developing optic lobe. According to previous studies, several glial subtypes were identified in the developing optic lobe (Fig. 4A and B) (Edwards and Meinertzhagen, 2010; Edwards et al., 2012; Hara et al., 2013). Therefore, to determine the glial subtypes required for clearance, we searched for GAL4 lines that specifically expressed GAL4 in glial subtypes in the developing optic lobe. Several GAL4 lines have been reported to express GAL4 in glial subtypes in the larval or adult brain (Awasaki et al., 2008; Doherty et al., 2009; Kremer et al., 2017). However, few data are available regarding the expression pattern of GAL4 in glial subtype-specific GAL4 lines in the developing optic lobe (Edwards et al., 2012), and a systematic study is needed.

Here, we described the expression pattern of GAL4 in several glial subtype-specific GAL4 lines during metamorphosis in the developing optic lobe (Fig. 5B, Table 1). Before the investigation, we confirmed the expression pattern of GAL4 in the adult central brain in each line and confirmed that the pattern was the same as previously reported (Awasaki et al., 2008; Doherty et al., 2009). Kremer et al. (2017) proposed a generic naming of adult optic lobe glia (Fig. 4B). However, there is now no standard naming on pupal optic lobe glia, because some inconsistencies have been observed between our previous studies (Togane, 2012; Hara et al., 2013) and Edwards et al. (2012) on the development of the lamina neuropil glia during metamorphosis (Fig. 4B). Therefore, the present study follows the naming system of Kremer et al. (2017) with minor modification based on Hara et al. (2013) (Fig. 4A and B).

The results showed that the expression pattern of GAL4 was greatly different in pupal stages compared to larval and adult stages and altered during metamorphosis (Fig. 5A and B). A summary table is given in Table 1. Glial cells were detected on the MLpL neuropil surface throughout pupal stages with anti-Repo antibody (Fig. 5A 24 h-2, arrowhead). However, no glial subtype GAL4 lines express GAL4 in these glial cells in the optic lobe at early pupal stages. Glial subtype GAL4 lines that specifically express GAL4 in astrocyte-like glia or ensheathing glia in the adult MLpL region began expression at late pupal stages or around eclosion. Therefore, glia on the MLpL neuropil surface at pupal stages are collectively called neuropil glia (NG) in the present study.

In NP2222 > mCD8-GFP (Fig. 5B), GFP was expressed in lamina distal cortex glia from 0 to 24 h APF in the lamina region, but the expression was weak at 48 and 72 h APF. In the MLpL region, GFP was expressed in cortex glia from 0 to 72 h APF. GFP expression in the cortex of the MLpL region overlapped only with repo-positive nuclei (cortex glia) in the cortex (Fig. 5C1, white arrow), but not with repo-positive nuclei (perineurial and subperineurial glia) on the surface of the MLpL region (Fig. 5C1, white arrowhead), or with repo-positive nuclei (neuropil glia, NG) on the lobula plate neuropil surface (Fig. 5C1, yellow arrowhead). Outer and inner chasm glia continued to express GFP from 0 to 72 h APF (Fig. 5B). GFP expression extending from outer chiasm glia along the medulla neuropil surface at 24 h APF did not overlap with repo-positive nuclei (neuropil glia, NG) on the medulla neuropil surface (Fig. 5C1', yellow arrowhead), suggesting that this expression was present in outer chiasm glia, but not neuropil glia (NG).

In NP1243 > mCD8-GFP (Fig. 5B), lamina distal cortex glia were labeled with GFP from 0 to 72 h APF in the lamina region (Fig. 5C3, yellow arrowhead). At 12 and 24 h APF, some larval marginal glia (L-ALG) began to express GFP (Fig. 5B, C3, yellow arrow). The expression subsequently increased and was observed in many lamina astrocyte-like glia and lamina ensheathing glia at 72 h APF (Fig. 5B). In the MLpL region, GFP was expressed in cortex glia from 0 to 12 h APF (Fig. 5B, B1). This expression did not overlap with repo-positive nuclei (perineurial

A

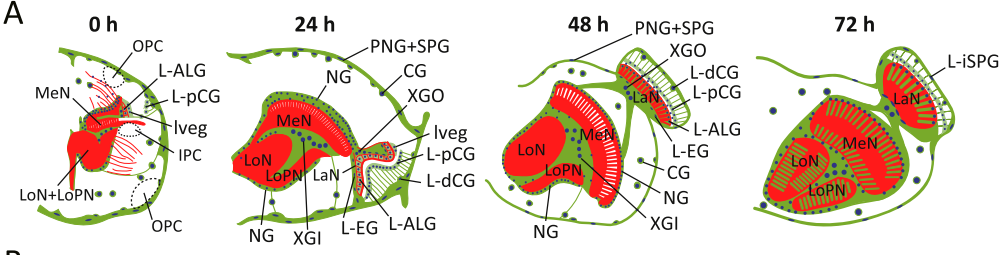

B

< Lamina region >

	present study pupa	Hara et al. (2013) pupa	Edwards et al. (2012) larva, pupa & adult	Kremer et al. (2017) generic adult
Surface	perineurial glia (PNG) (*l)	perineurial glia (*l)	perineurial glia (*l) fenestrated glia (*a)	
	subperineurial glia (SPG) (*l) lamina interface subperineurial glia (L-iSPG) (*a)	subperineurial glia (*l) pseudocartridge glia (*a)	subperineurial glia (*l) pseudocartridge glia (*a)	lamina interface subperineurial glia (L-iSPG) (*a)
Cortex	lamina distal cortex glia (L-dCG) (*l, *a)	distal satellite glia (*a)	wrapping glia (*le) distal satellite glia (*a)	lamina distal cortex glia (L-dCG) (*a)
	lamina proximal cortex glia (L-pCG) (*l, *a)	proximal satellite glia (*l, *a)	proximal satelite glia (*l, *a)	lamina proximal cortex glia (L-pCG) (*a)
Neuropil	larval epithelial glia (lveg) (*l) larval marginal glia (L-ALG) (*l, *a)	larval epithelial glia (*l) larval marginal glia (*l, *a)	epithelial glia (*l, *a)	lamina astrocyte-like glia (L-ALG) (*a)
	lamina ensheathing glia (L-EG) (*a)	adult marginal glia (*a)	marginal glia (*l, *a)	lamina ensheathing glia (L-EG) (*a)

< Medulla, Lobula and Lobula plate region >

	present study pupa	Hara et al. (2013) pupa	Edwards et al. (2012) larva, pupa & adult	Kremer et al. (2017) generic adult
Surface	perineurial glia (PNG) (*l, *a)	perineurial glia (*l, *a)	perineurial glia (*l, *a)	perineurial glia (PNG) (*a)
	subperineurial glia (SPG) (*l, *a)	subperineurial glia (*l, *a)	subperineurial glia (*l, *a)	subperineurial glia (SPG) (*a)
Cortex	cortex glia (CG) (*l, *a)	satellite glia (*l, *a)	satellite glia (*l, *a)	cortex glia (CG) (*a)
Neuropil	neuropil glia (NG) (*l)	neuropil glia (*l, *a)	neuropil glia (*l)	
	astrocyte-like glia (ALG) (*a)		several subtypes of neuropil glia (*a)	astrocyte-like glia (ALG) (*a)
	ensheathing glia (EG) (*a)			ensheathing glia (EG) (*a)

< Chiasm region >

	present study pupal	Hara et al. (2013) pupa	Edwards et al. (2012) larva, pupa & adult	Kremer et al. (2017) generic adult
Chiasma	outer chiasm glia (XGO) (*l, *a)	outer chiasmal glia (*l, *a)	outer chiasm giant glia (*l, *a)	outer chiasm glia (XGO) (*a)
	inner chiasm glia (XGI) (*l, *a)	inner chiasmal glia (*l, *a)	inner chiasm giant glia (*l, *a)	inner chiasm glia (XGI) (*a)

*l: larva and early pupa *a: adult and late pupa *le: larval eye disc

Fig. 4. Nomenclature and abbreviations of glia subtypes in the developing optic lobe. (A) Schematic drawings of the developing optic lobe and the distribution of glia subtypes. Green: glial cytoplasm. Glial cytoplasm in a mesh-like and a centripetal pattern in the cortices is omitted. Red: neuropil. Blue: Glial nuclei. Two types of surface glia, perineurial glia (PNG) and subperineurial glia (SPG), were not distinguished in the developing optic lobe in the medulla, lobula plate, and lobula (MLpL) region. Therefore, they are named perineurial and subperineurial glia (PNG + SPG) here. (B) Comparison of nomenclature of glia subtypes among the present and previous studies. Kremer et al. (2017) proposed a naming system for glia, generic glia, in the adult optic lobe. Edwards et al. (2012), Togane (2012), Hara et al. (2013) and Chen et al. (2016) described, in detail, the development of lamina neuropil glia during metamorphosis. Larval epithelial glia and larval marginal glia develop from a common progenitor cells. However, some inconsistencies have been observed between our previous studies (Togane, 2012; Hara et al., 2013) and Edwards et al. (2012) on the development of these glia during metamorphosis. The present study, then, follows the naming system of Kremer et al. (2017) with minor modification based on our previous studies (Togane, 2012; Hara et al., 2013, Fig. 4A). Larval marginal glia develop into adult epithelial glia (lamina astrocyte glia, L-ALG), but not into adult marginal glia. Therefore, the abbreviation L-ALG is used for larval marginal glia as well as for adult epithelial glia. Larval epithelial glia (lveg) disappear from the original place during 6–24 h APF. Adult marginal glia (L-EG) does not develop from larval marginal glia, but from small glia observed at early pupal stages on the boundary between the lamina neuropil and the outer chiasm. Therefore, the abbreviation L-EG is used for these small glia as well as for adult marginal glia.

and subperineurial glia) on the surface of the MLpL region (Fig. 5C2, white arrowhead), but did overlap with repo-positive nuclei (cortex glia) in the cortex near the surface layer (Fig. 5C2, white arrow). GFP expression in cortex glia weakened and disappeared by 24 h APF (Fig. 5B). Expression in neuropil glia (NG) at 48 h APF began in a few cells on the lobula plate neuropil surface (Fig. 5B). This expression spread thereafter and was observed in neuropil glia (NG) on the MLpL neuropil surface at 72 h APF. In addition, we noted that GFP-positive thin protrusions extended into the neuropil from neuropil glia.

In NP0577 > mCD8-GFP (Fig. 5B), GFP was expressed quite weakly in the cortex in the lamina region at 0 h APF. This expression disappeared at 24 h APF. Thereafter, weak GFP expression began again in lamina proximal cortex glia at 48 h APF and become stronger in lamina distal cortex glia, lamina astrocyte-like glia, and lamina ensheathing glia at 72 h APF. In the MLpL region, GFP was quite weakly expressed in cortex glia at 0 h APF (Fig. 5B). At 24 h APF, stronger expression was only observed in cortex glia near the optic lobe surface. This expression then increased and expanded to cortex glia across the cortex at 48 and 72 h APF. The expression overlapped with repo-positive nuclei (cortex glia) in the medulla, lobula plate, and lobula cortices (Fig. 5C4, 5, arrows), but did not overlap with repo-positive nuclei (perineurial and subperineurial glia) on the surface of the MLpL region (Fig. 5C4, 5, white arrowhead), or with repo-positive nuclei (neuropil glia, NG) on the MLpL neuropil surface (Fig. 5C4, 5, yellow arrowhead). In outer and inner chiasm glia, GFP expression began at 48 h APF and became moderate at 72 h APF (Fig. 5B).

In NP3233 > mCD8-GFP (Fig. 5B), *alrm-GAL4*>mCD8-GFP (Fig. 5B) and NP6520 > mCD8-GFP (Fig. 5B2), GFP was expressed in outer and inner chiasm glia and/or neuropil glia, but not in cortex glia. Detailed expression was described in the Table 1 legend.

In NP6293 > mCD8-GFP (Fig. 5B) and NP2276 > mCD8-GFP

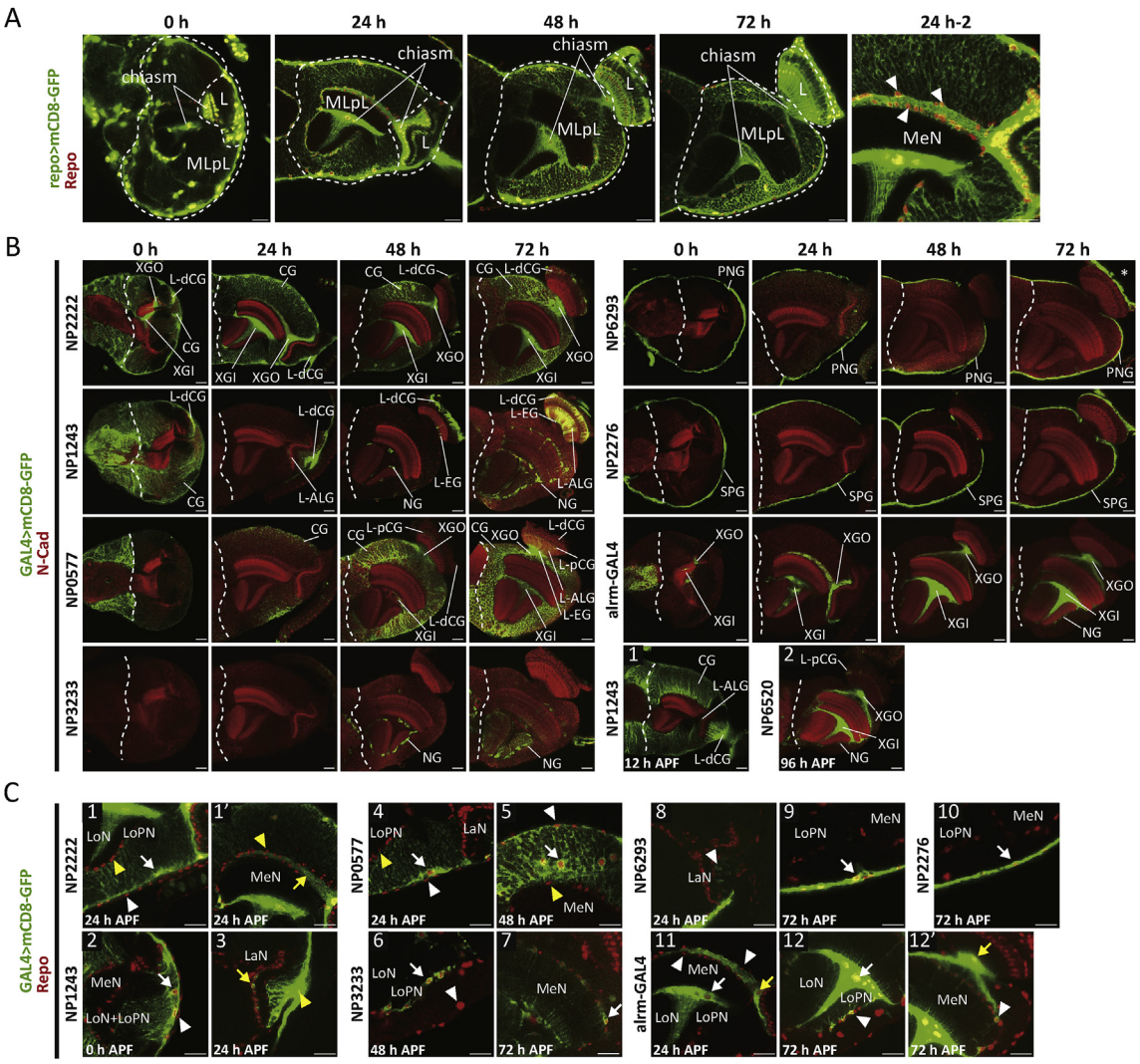

Fig. 5. Expression pattern of GAL4 in glial subtype GAL4 lines in the developing optic lobe. (A) GFP pattern in *UAS-mCD8::GFP/+; repo-GAL4/+* during metamorphosis. Green: mCD8-GFP, Red: anti-Repo. Dorsal view. MLpL: medulla, lobula plate, and lobula region, L: lamina region, chiasm: outer and inner chiasm. 24 h-2: A magnified image of the optic lobe at 24 h APF. arrowheads: neuropil glia (NG) around the medulla neuropil. MeN: medulla neuropil. (B) GFP pattern during metamorphosis in *NP2222/UAS-mCD8::GFP*, *NP1243/UAS-mCD8::GFP*, *NP0577/+* or Y; *UAS-mCD8::GFP/+*, *UAS-mCD8::GFP/+*; *NP3233/+*, *NP6293/UAS-mCD8::GFP*, *NP2276/UAS-mCD8::GFP*, *alrm-GAL4/UAS-mCD8::GFP*, and *UAS-mCD8::GFP/+*; *NP6520/+*. Green: mCD8-GFP, Red: anti-N-cadherin. (C) Glial nuclei and GFP pattern in the same genotypes as in (B). Green: mCD8-GFP, Red: anti-Repo. (1-1′): NP2222 at 24 h APF. White arrow: cortex glia (CG). White arrowhead: perineurial and subperineurial glia (PNG + SPG). Yellow arrowhead: neuropil glia (NG). Yellow arrow: cytoplasm of outer chiasm glia (XGO). (2–3): NP1243 at 0 h and 24 h APF. White arrow: cortex glia (CG). White arrowhead: perineurial and subperineurial glia (PNG + SPG). Yellow arrow: larval marginal glia (L-ALG). Yellow arrowhead: lamina-distal cortex glia (L-dCG). (4–5): NP0577 at 24 h and 48 h APF. White arrow: cortex glia (CG). White arrowhead: perineurial and subperineurial glia (PNG + SPG). Yellow arrowhead: neuropil glia (NG). (6–7): NP3233 at 48 h and 72 h APF. Arrow: neuropil glia (NG). Arrowhead: cortex glia (CG). GFP overlapped with neuropil glia (NG) in the lobula plate cortex (LoPC) at 48 h APF. Cytoplasmic protrusion from neuropil glia (NG) extends into the medulla neuropil (MeN) at 72 h APF. (8–9): NP6293 at 24 h and 72 h APF. Arrowhead: GFP-expressing neurons in the lamina region at 24 h APF. Arrow: perineurial and subperineurial glia (PNG + SPG). (10): NP2276 at 72 h APF. Arrow: perineurial and subperineurial glia (PNG + SPG). (11–12′): alrm-*GAL4* at 24 h and 72 h APF. White arrow: inner chiasm glia (XGI). Yellow arrow: outer chasm glia (XGO). Arrowhead: neuropil glia (NG). GFP did not overlap with neuropil glia (NG) on the MeN surface at 24 h APF, but did overlap at 72 h APF. Thin cytoplasmic protrusions extended from neuropil glia (NG) into the MLpL neuropil at 72 h APF.

(Fig. 5B), GFP was expressed in perineurial glia or subperineurial glia. Detailed expression was described in the Table 1 legend.

As a result, we identified GAL4 lines that specifically drive gene expression in one or a few glial subtypes in the developing optic lobe (Table 1). However, we did not identify GAL4 lines for neuropil glia in the MLpL region, larval epithelial glia (lveg) in the lamina region, larval marginal glia (L-ALG) in the lamina region, or lamina entheathing glia (L-EG) in the lamina region at early pupal stages.

2.5. *Drpr expression in cortex glia is necessary and sufficient for clearing dead young neurons in the developing optic lobe*

Before analyzing the function of glial subtypes in dead cell clearance, we confirmed Drpr expression in glial subtypes with the anti-Drpr antibody. The results showed that Drpr was expressed in all glial subtypes: cortex glia (Fig. 6A1, 5, 6), outer and inner chiasm glia (Fig. 6A1), perineurial and subperineurial glia (Fig. 6A2), neuropil glia (NG) (Fig. 6A3, 4), lamina distal cortex glia (L-dCG, Fig. 6A5-8), lamina entheathing glia

Table 1
The expression pattern of glia subtype GAL4s in the developing optic lobe.

GAL4	region	developmental stage (h APF)					
		0 h	12 h	24 h	48 h	72 h	96 h
NP2222	L	L-dCG	*	L-dCG	L-dCG	L-dCG	*
	MLpL	CG	*	CG	CG	CG	*
	Chiasm	XGO, XGI	*	XGO, XGI	XGO, XGI	XGO, XGI	*
NP1243	L	L-dCG	L-dCG, L-ALG, L-EG	L-dCG, L-ALG, L-EG	L-dCG, L-ALG, L-EG	L-dCG, L-ALG, L-EG	*
	MLpL	CG	CG		NG	NG	*
	Chiasm						*
NP0577	L	(L-dCG, L-pCG)	*		L-dCG, L-pCG	L-dCG, L-pCG, L-ALG, L-EG	*
	MLpL	(CG)	*	CG	CG	CG	*
	Chiasm		*		XGO, XGI	XGO, XGI	*
NP3233	L		*				*
	MLpL		*		NG	NG	*
	Chiasm		*				*
NP6293	L	PNG	*	PNG (part), (neuron)			*
	MLpL	PNG	*	PNG	PNG	PNG	*
	Chiasm		*				*
NP2276	L	SPG	*			SPG	*
	MLpL	SPG	*	SPG	SPG	SPG	*
	Chiasm		*				*
alrm-GAL4	L		*				*
	MLpL		*			NG	*
	Chiasm	XGO, XGI	*	XGO, XGI	XGO, XGI	XGO, XGI	*
NP6520	L		*				L-pCG
	MLpL		*				NG
	Chiasm		*				XGO, XGI
repo-GAL4	L	L-dCG, L-pCG, L-ALG, lveg, PNG, SPG	L-dCG, L-pCG, L-EG, L-ALG, lveg, PNG, SPG	L-dCG, L-pCG, L-EG, L-ALG, lveg, PNG, SPG	L-dCG, L-pCG, L-EG, L-ALG, PNG, SPG	L-dCG, L-pCG, L-EG, L-ALG, PNG, SPG	L-dCG, L-pCG, L-EG, L-ALG, PNG, SPG
	MLpL	CG, NG, PNG, SPG	CG, NG, PNG, SPG	CG, NG, PNG, SPG	CG, NG, PNG, SPG	CG, NG, PNG, SPG	CG, NG, PNG, SPG
	Chiasm	XGO, XGI	XGO, XGI	XGO, XGI	XGO, XGI	XGO, XGI	XGO, XGI

*: not examined, ( ): weak expression, (neuron): several lamina neurons.

In NP3233 > mCD8-GFP (Fig. 5B), GFP expression was not observed throughout the optic lobe at 0 or 24 h APF. However, in the MLpL region, the expression started in neuropil glia (NG) at 48 h APF and was strong at 72 h APF. Expression was also seen in cytoplasmic protrusions that extended into the neuropil from neuropil glia (NG). This expression did not overlap with repo-positive nuclei (cortex glia) in the lobula plate cortex (Fig. 5C6, arrowhead), but overlapped with repo-positive nuclei (neuropil glia, NG) on the lobula plate neuropil surface (Fig. 5C6, 6', arrow).

In *alrm-GAL4*>mCD8-GFP (Fig. 5B), GFP expression was observed in outer and inner chiasm glia from 0 to 72 h APF. GFP expression extending from outer chiasm glia did not overlap with repo-positive nuclei (neuropil glia, NG) on the medulla neuropil surface (Fig. 5C11, arrowhead). In addition, at 48 h APF, GFP expression started in a few neuropil glia (NG) on the MLpL neuropil surface (Fig. 5B), and the number of GFP-expressing neuropil glia (NG) increased through 72 h APF. Many GFP-labeled cytoplasmic protrusions were observed invading the neuropil from neuropil glia (NG) at 72 h APF (Fig. 5C12, 12′, arrowhead).

In NP6520 > mCD8-GFP, GFP was not expressed in any cells from 0 to 72 h APF, but began to be expressed at 96 h APF in L-pCG, neuropil glia (NG), outer and inner chiasm glia and cytoplasmic protrusions from neuropil glia (NG) (Fig. 5B2).

According to previous studies (Awasaki et al., 2008), NP6293 is a driver that is specific for perineurial glia, and NP2276 is specific for subperineurial glia. In this study, we observed that GFP was expressed in glia on the optic lobe surface in both NP6293 > mCD8-GFP and NP2276 > mCD8-GFP. No difference was observed in the expression pattern between them on the surface of the MLpL region (Fig. 5B, C9, 10, arrows). However, NP2276 was expressed on the surface of the lamina region at 72 h APF, but not NP6293 (Fig. 5B).

In NP6293 > mCD8-GFP (Fig. 5B), GFP was expressed in perineurial glia at 0 h APF in the lamina region. This expression began to disappear by 24 h APF, and no expression was seen in the lamina region thereafter. Additionally, temporary weak expression was observed in some lamina neurons at 24 h APF but not after 48 h APF (Fig. 5C8, arrowhead). In the MLpL region, GFP expression was observed in perineurial glia from 0 to 72 h APF (Fig. 5C9, arrow).

In NP2276 > mCD8-GFP (Fig. 5B), GFP was expressed in subperineurial glia at 0 h APF in the lamina region, but the expression disappeared by 24 h APF. However, it appeared again, and strong expression was observed at 72 h APF. In the MLpL region, GFP was expressed in subperineurial glia from 0 to 72 h APF (Fig. 5B, C10, arrow).

In *repo-GAL4>mCD8-GFP* (Fig. 5A), GFP was expressed in all subtypes of glia throughout the pupal period, though a few cortex and neuropil glia cells in the medulla region did not express GFP at early pupal periods. GFP expression in the adult at 120 h APF was the same as in the late pupa at 72 h APF or 96 h APF in all lines.

(L-EG, Fig. 6A6), larval marginal glia (L-ALG, Fig. 6A7), and lamina proximal cortex glia (L-pCG, Fig. 6A8).

We performed knockdown of *drpr* using the glial subtype-specific GAL4s and analyzed the number of TUNEL-positive cells that accumulated in the optic lobe. Results were different between the MLpL region and lamina region. In the MLpL region, numerous TUNEL-positive cells accumulated in NP2222>*drpr*-RNAi and NP1243>*drpr*-RNAi (Fig. 6B and C). Glial subtypes in which both NP2222 and NP1243 drive gene expression at early pupal stages were cortex glia in the MLpL region (Fig. 5B, Table 1), and thus, *drpr* expression in cortex glia at early pupal stages was necessary for dead cell clearance. In contrast, *drpr* knockdown using NP3233, NP6293, NP2276, or *alrm-GAL4* showed no increase in the number of dead cells compared to the wild type (Fig. 6C). As NP6293, NP2276, and a*lrm-GAL4* drive genes in perineurial and subperineurial glia, or outer and inner chiasm glia from 0 to 24 h APF, but not in cortex glia (Fig. 5B, Table 1), perineurial and subperineurial glia or outer and inner chiasm glia were not necessary for dead cell clearance. *drpr* knockdown with NP0577 did not increase the number of dead cells (Fig. 6C). In contrast to NP2222 and NP1243, NP0577 drives gene expression only quite weakly in cortex glia at 0 h APF and in a small number of cortex glia at 24 h APF as described in the previous section (Fig. 5B, Table 1). The above result is consistent with the idea that *drpr* expression at late third larval and early pupal stages is necessary for dead cell clearance, but not at later stages. No GAL4 lines are available for neuropil glia (NG) at early pupal stages (Fig. 5B, Table 1), and thus, the necessity for this glial subtype in dead cell clearance remains unclear.

There was no glial subtype-specific GAL4>drpr-RNAi in which numerous TUNEL-positive cells accumulated in the lamina region. Both NP2222 and NP1243 drive gene expression at early pupal stages in lamina distal cortex glia (Fig. 5B, Table 1), and thus, *drpr* expression in lamina distal cortex glia at early pupal stages was not necessary for dead cell clearance. The necessity for drpr expression in lamina proximal cortex glia (L-pCG) in dead cell clearance is described in a later section. No GAL4 lines are available for larval epithelial glia (lveg) or larval marginal glia (L-ALG) at early pupal stages (Fig. 5B, Table 1), and thus, the necessity for these glial subtypes in dead cell clearance remains unclear.

To confirm the effect of glial subtype RNAi on Drpr expression, we examined Drpr expression in NP2222>*drpr*-RNAi and NP1243>*drpr*-

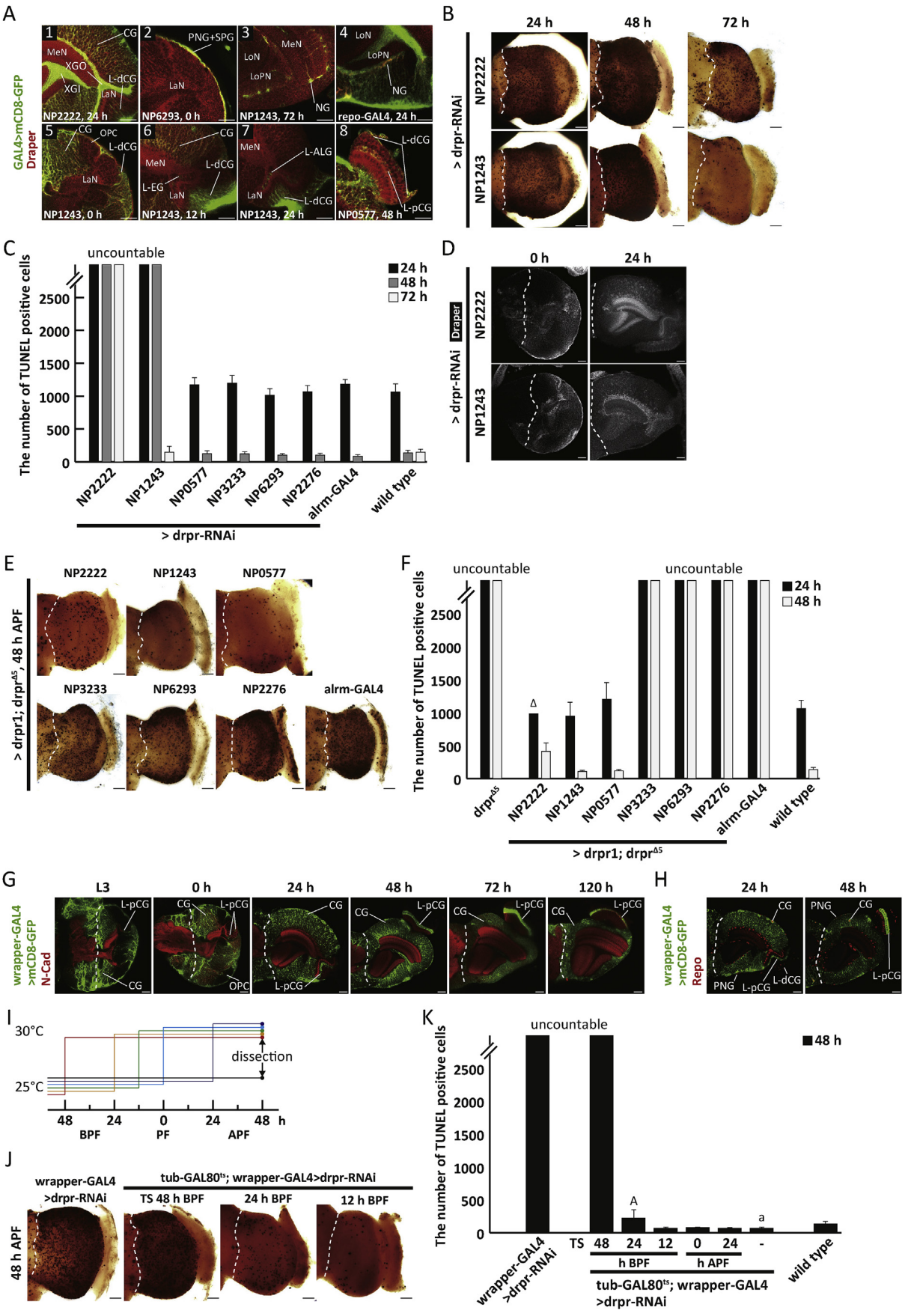

(caption on next page)

Fig. 6. Cortex glia and lamina cortex glia are required for dead cell clearance in the optic lobe. (A) Draper expression in glia subtypes. Green: mCD8-GFP, Red: anti-Drpr. (1) *NP2222/UAS-mCD8::GFP* at 24 h APF. (2) *NP6293/UAS-mCD8::GFP* at 0 h APF. (3, 5, 6, 7) *NP1243/UAS-mCD8::GFP* at 72 h, 0 h, 12 h, and 24 h APF. (4) *UAS-mCD8::GFP/+*; *repo-GAL4/+* at 24 h APF. (8) *NP0577/+* or Y; *UAS-mCD8::GFP/+* at 48 h APF. (B) TUNEL-positive cells in optic lobes in *NP2222/UAS-draper*-RNAi, *NP1243/UAS-draper*-RNAi. (C) The number of TUNEL-positive cells in optic lobes in *NP2222/UAS-draper*-RNAi, *NP1243/UAS-draper*-RNAi, *NP0577/+* or Y; *UAS-draper*-RNAi/+, *UAS-draper*-RNAi/+; *NP3233/+*, *NP6293/UAS-draper*-RNAi, *NP2276/UAS-draper*-RNAi, *alrm-GAL4/UAS-draper*-RNAi. The number of TUNEL-positive cells in *NP2222/UAS-draper*-RNAi and *NP1243/UAS-draper*-RNAi was uncountable. No significant difference was found in the other *GAL4s > draper*-RNAi in comparison with the wild type. Mean ± SD. n = 10 in the wild type and n = 5 in *GAL4s > draper*-RNAi. $P < 0.05$ (Kruskal-Wallis rank sum test and post hoc Wilcoxon rank sum test with Bonferroni correction). (D) Draper expression in *NP2222/UAS-draper*-RNAi and *NP1243/UAS-draper*-RNAi. White: anti-Draper. (E) TUNEL-positive cells in optic lobes in $drpr^{\Delta 5}/drpr^{\Delta 5}$, *NP2222/UAS-draper1*; $drpr^{\Delta 5}/drpr^{\Delta 5}$, *NP1243/UAS-draper1*; $drpr^{\Delta 5}/drpr^{\Delta 5}$, *NP0577/+* or Y; *UAS-draper1/+*; $drpr^{\Delta 5}/drpr^{\Delta 5}$, *UAS-draper1/+*; *NP3233* $drpr^{\Delta 5}/drpr^{\Delta 5}$, *NP6293/UAS-draper1*, $drpr^{\Delta 5}/drpr^{\Delta 5}$, *NP2276/UAS-draper1*; $drpr^{\Delta 5}/drpr^{\Delta 5}$ and *alrm-GAL4/UAS-draper1*; $drpr^{\Delta 5}/drpr^{\Delta 5}$. (F) The number of TUNEL-positive cells in optic lobes in the same genotypes as in (E). The number of TUNEL-positive cells was uncountable in $drpr^{\Delta 5}/drpr^{\Delta 5}$, *UAS-draper1/+*, *NP3233* $drpr^{\Delta 5}/drpr^{\Delta 5}$, *NP6293/UAS-draper1*; $drpr^{\Delta 5}/drpr^{\Delta 5}$, *NP2276/UAS-draper1*; $drpr^{\Delta 5}/drpr^{\Delta 5}$, and *alrm-GAL4/UAS-draper1*; $drpr^{\Delta 5}/drpr^{\Delta 5}$. No significant difference was found in the other *GAL4s > draper1*; $drpr^{\Delta 5}/drpr^{\Delta 5}$ in comparison with the wild type. Mean ± SD. n = 10 in the wild type and n = 5 in *GAL4s > draper*-RNAi (n = 1 in Δ). $P < 0.05$ (Kruskal-Wallis rank sum test and post hoc Wilcoxon rank sum test with Bonferroni correction). (G) GFP pattern in *UAS-mCD8::GFP/+*; *wrapper-GAL4/+* during metamorphosis. Green: mCD8-GFP, Red: anti-N-Cad. (H) GFP pattern in *UAS-mCD8::GFP/+*; *wrapper-GAL4/+*. Green: mCD8-GFP, Red: anti-Repo. (I) Scheme of temperature shift for $GAL80^{ts}$ experiments. BPF: before puparium formation. (J) TUNEL positive cells in *UAS-draper*-RNAi/+; *wrapper-GAL4/+* and *tub-*$GAL80^{ts}$*/UAS-draper*-RNAi; *wrapper-GAL4/+*. Pupae at 48 h APF were dissected and stained. TS 48 h, 24 h and 12 h BPF: temperature shift at 48 h, 24 h and 12 h BPF. (K) The number of TUNEL positive cells in *UAS-drpr*-RNAi/+; *wrapper-GAL4/+* and *tub-*$GAL80^{ts}$*/UAS-draper*-RNAi; *wrapper-GAL4/+*. The number of TUNEL-positive cells was uncountable in *UAS-draper*-RNAi/+; *wrapper-GAL4/+* and in TS 48 h BPF *tub-*$GAL80^{ts}$*/UAS-draper*-RNAi; *wrapper-GAL4/+*. A in TS 24 h BPF *tub-*$GAL80^{ts}$*/UAS-draper*-RNAi; *wrapper-GAL4/+* were significantly different from a in no temperature shift (at 25 °C) control. No significant difference was found in the other *tub-*$GAL80^{ts}$*/UAS-draper*-RNAi; *wrapper-GAL4/+*. Mean ± SD. n = 6–9. $P < 0.05$ (Kruskal-Wallis rank sum test and post hoc Wilcoxon rank sum test with Bonferroni correction).

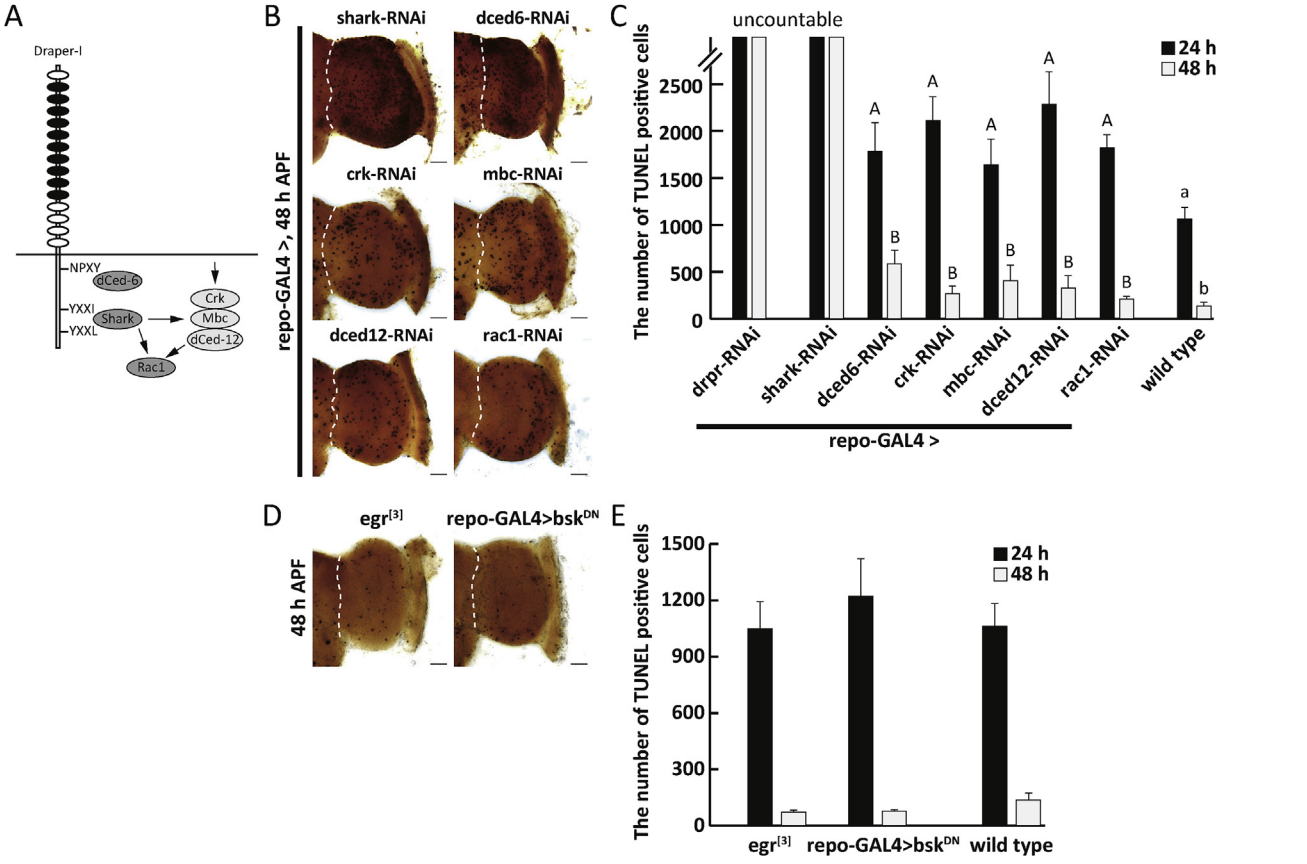

Fig. 7. Signaling molecules downstream of Drpr function to clear dead cells in the optic lobe. (A) A schematic of the signaling pathway downstream of Drpr (Ziegenfuss et al., 2012). (B) TUNEL-positive cells in optic lobes in *repo-GAL4/UAS-shark*-RNAi, *UAS-dced6*-RNAi/+; *repo-GAL4/+*, *UAS-crk*-RNAi/+; *repo-GAL4/+*, *repo-GAL4/UAS-mbc*-RNAi, *repo-GAL4/UAS-dced12*-RNAi, and *UAS-rac1*-RNAi/+; *repo-GAL4/+*. (C) The number of TUNEL positive cells in optic lobes in *UAS-draper*-RNAi/+; *repo-GAL4/+* and *repo-GAL4/UAS-shark*-RNAi was uncountable. A and B in the other *repo-GAL4>genes*-RNAi are significantly different from a and b in the wild type, respectively. Mean ± SD. n = 10 in the wild type and n = 5 in *repo-GAL4>genes*-RNAi. $P < 0.05$ (Kruskal-Wallis rank sum test and post hoc Wilcoxon rank sum test with Bonferroni correction). (D) TUNEL-positive cells in $egr^{[3]}/egr^{[3]}$ and *UAS-*bsk^{DN}*/+* or Y; *repo-GAL4/+* optic lobes. (E) The number of TUNEL-positive cells in $egr^{[3]}/egr^{[3]}$ and *UAS-*bsk^{DN}*/+* or Y; *repo-GAL4/+* optic lobes. $egr^{[3]}/egr^{[3]}$ and *repo-GAL4>*bsk^{DN} were not significantly different from samples in the wild type. Mean ± SD. n = 10 in the wild type and n = 5 in $egr^{[3]}/egr^{[3]}$ and *UAS-*bsk^{DN}*/+* or Y; *repo-GAL4/+*. $P < 0.05$ (Kruskal-Wallis rank sum test and post hoc Wilcoxon rank sum test with Bonferroni correction).

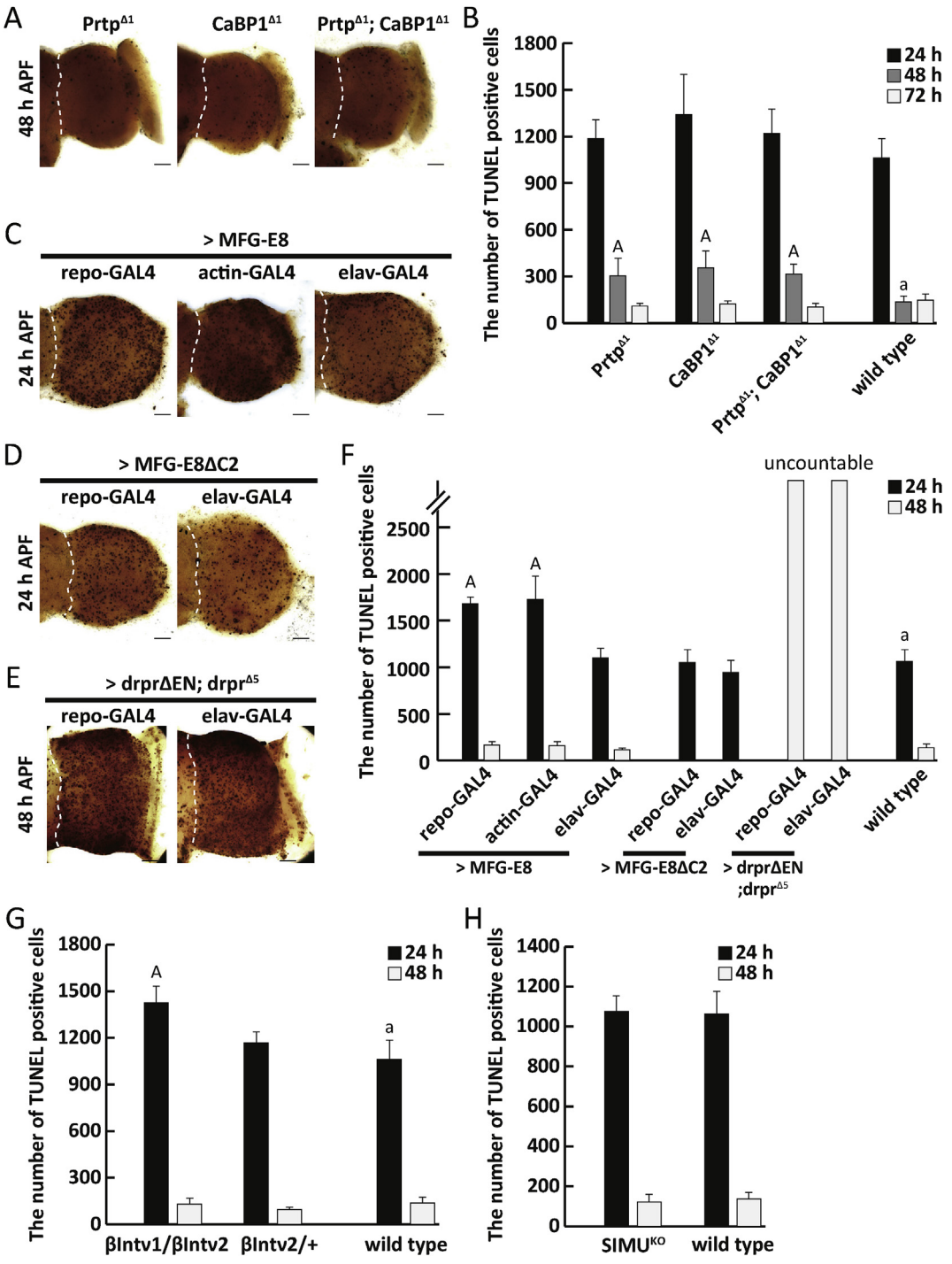

Fig. 8. Drpr ligand candidates, Pretaporter, CaBP1, and phosphatidylserine, function to clear cell bodies of dead neurons. (A) TUNEL-positive cells in *Prtp$^{\Delta 1}$/Prtp$^{\Delta 1}$*, *CaBP1$^{\Delta 1}$/CaBP1$^{\Delta 1}$*, and *Prtp$^{\Delta 1}$/Prtp$^{\Delta 1}$*; *CaBP1$^{\Delta 1}$/CaBP1$^{\Delta 1}$*. (B) The number of TUNEL-positive cells in the same genotypes and the wild type. A in mutants is significantly different in comparison with a in the wild type. The other samples in mutants were not significantly different from samples in the wild type. Mean ± SD. n = 10 in the wild type and n = 5 in mutants. P < 0.05 (Kruskal-Wallis rank sum test and post hoc Wilcoxon rank sum test with Bonferroni correction). (C, D, E) TUNEL-positive cells in optic lobes in *UAS-MFG-E8/+*; *repo-GAL4/+*, *actin-GAL4/UAS-MFG-E8*, *elav-GAL4/+* or Y; *UAS-MFG-E8/+*, *UAS-MFG-E8ΔC2/+*; *repo-GAL4/+*, *elav-GAL4/+* or Y; *UAS-MFG-E8ΔC2/+*, *UAS-draperΔEN/+*; *repo-GAL4 drpr$^{\Delta 5}$/drpr$^{\Delta 5}$*, and *elav-GAL4/+* or Y; *UAS-draperΔEN/+*; *drpr$^{\Delta 5}$/drpr$^{\Delta 5}$*. (F) The number of TUNEL-positive cells in optic lobes in the same genotypes as in (C, D, E) in which *drprΔEN* was forced to be expressed on the *drpr* mutant background using tissue-specific *GAL4s*. The number of TUNEL-positive cells in *UAS-draperΔEN/+*; *repo-GAL4 drpr$^{\Delta 5}$/drpr$^{\Delta 5}$* and *elav-GAL4/+* or Y; *UAS-draperΔEN/+*; *drpr$^{\Delta 5}$/drpr$^{\Delta 5}$* was uncountable. A in *GAL4>MFG-E8* at 24 h APF was significantly different from the wild type. The other samples in *GAL4>MFG-E8* and *GAL4>MFG-E8ΔC2* were not significantly different from samples in the wild type. Mean ± SD. n = 10 in the wild type and n = 5 in transgenic flies. P < 0.05 (Kruskal-Wallis rank sum test and post hoc Wilcoxon rank sum test with Bonferroni correction). (G) The number of TUNEL-positive cells in *β-Int ν1/β-Int ν2,* and *β-Int ν2/+* optic lobes. A in *β-Int ν1/β-Int ν2* at 24 h APF was significantly different from a in the wild type. The other samples in mutants were not significantly different from correspondent samples in the wild type. Mean ± SD. n = 10 in the wild type and n = 5 in mutants. P < 0.05 (Kruskal-Wallis rank sum test and post hoc Wilcoxon rank sum test with Bonferroni correction). (H) The number of TUNEL-positive cells in *SIMU ^{KO}/SIMU ^{KO}* optic lobes. Samples in the mutant were not significantly different from correspondent samples in the wild type. Mean ± SD. n = 10 in the wild type and n = 5 in the mutant. P < 0.05 (Kruskal-Wallis rank sum test and post hoc Wilcoxon rank sum test with Bonferroni correction).

RNAi with anti-Drpr antibody (Fig. 6D). The results showed that in NP2222>*drpr*-RNAi, Drpr expression was markedly decreased in the MLpL cortex and the inner chiasm in comparison to the wild type at all stages. Drpr expression in the surface layer of the lamina region and in the outer chiasm disappeared at 24 h APF. In contrast, spotted staining appeared at 24 h APF in the medulla cortex as in *repo-GAL4*>*drpr*-RNAi. Drpr expression remained in the OPC, lamina cortex and outer and inner chiasm at 0 h APF, and in the lamina cortex, lamina neuropil, MLpL neuropil, and MLpL neuropil surface at 24 h APF. In NP1243>*drpr*-RNAi, Drpr expression in the MLpL cortex and MLpL neuropil was markedly weaker than in the wild type at 0 h and 24 h APF stages. Drpr expression in the surface layer of the MLpL region was decreased at 24 h APF. However, spotted staining in the medulla cortex appeared at 24 h APF. Drpr expression remained in the OPC, IPC, lamina cortex, and outer and inner chiasm at 0 h APF, and in the lamina cortex, lamina neuropil, MLpL neuropil surface, and outer and inner chiasm at 24 h APF. Therefore, we confirmed that *drpr* knockdown with both NP2222 and NP1243 effectively reduced Drpr expression in cortex glia in the MLpL region, in agreement with the defect in dead cell clearance. We could not determine whether *drpr* knockdown with these GAL4 lines reduced Drpr expression in lamina distal cortex glia as there is a non-specific anti-Drpr staining in the lamina cortex as described in a previous section (Fig. 3A).

To further define the function of Drpr that is expressed in glial subtypes in dead cell clearance, we investigated whether dead cell clearance was rescued by forced expression of *drpr1* using different subtype GAL4s on the *drpr* mutant background. The results showed that the clearance was rescued when we used NP2222, NP1243, or NP0577 (Fig. 6E and F). Clearance was restored to almost the same level as in the wild type with NP2222, NP1243, and NP0577 at 24 and 48 h APF. In all these GAL4s, gene expression at early pupal stages was driven in cortex glia in the MLpL region and lamina distal cortex glia in the lamina region (Fig. 5B, Table 1). Therefore, these results suggest that cortex glia in the MLpL region and lamina distal cortex glia in the lamina region perform dead cell clearance. On the other hand, NP2222 did not force *drpr1* expression in larval epithelial glia (lveg), lamina proximal cortex glia, larval marginal glia (L-ALG), lamina entheathing glia (L-EG), or neuropil glia (NG) (Fig. 5B, Table 1). NP1243 did not force *drpr1* expression in larval epithelial glia (lveg), lamina proximal cortex glia, larval marginal glia (L-ALG), or neuropil glia (NG). NP0577 did not force *drpr1* expression in larval epithelial glia (lveg) or neuropil glia (NG). Thus, Drpr expression in larval epithelial glia (lveg), larval marginal glia (L-ALG), lamina proximal cortex glia, and lamina entheathing glia (L-EG) in the lamina region and in neuropil glia (NG) in the MLpL region is not requited for dead cell clearance. Moreover, forced expression of *drpr1* with NP3233, NP6293, NP2276, or *alrm-GAL4* did not rescue the clearance (Fig. 6E and F). In NP6293, NP2276 and *alrm-GAL4, drpr1* expression was driven in perineurial glia, subperineurial glia, or outer and inner chiasm glia (Fig. 5B, Table 1). Therefore, perineurial and subperineurial glia, and outer and inner chiasm glia do not perform dead cell clearance.

Altogether, we concluded that Drpr expression in cortex glia was necessary and sufficient to remove cell bodies of dead neurons in the MLpL region in the developing optic lobe. In the lamina region, lamina distal cortex glia performed dead cell clearance when *drpr1* was forced to express (Fig. 6E). However, lamina distal cortex glia was not essential for clearance (Fig. 6B). Considering that *repo* > *drpr*-RNAi suppressed dead cell clearance in the lamina region (Fig. 3C), it is suggested that another lamina cortex glia worked for dead cell clearance together (redundantly) with distal lamina cortex glia in the lamina region.

Recently a cortex glia-specific GAL4, *wrapper-GAL4* (GMR54H02), was reported (Kremer et al., 2017). Then, we corroborated the previous results using this GAL4. In *wrapper-GAL4*, GAL4 expressed in cortex glia in the MLpL region of the optic lobe at larval, pupal and adult stages (Fig. 6G). In the lamina region, GAL4 was expressed in a few cells near the posterior boundary of the lamina cortex in the larva. At pupal and adult stages, GAL4 was strongly expressed in lamina proximal cortex glia (Fig. 6G).

First, we examined the role of *drpr* expression in cortex glia and lamina proximal cortex glia in dead cell clearance using *wrapper* > *drpr*-RNAi. The result showed that *wrapper* > *drpr*-RNAi suppressed dead cell clearance in the MLpL region (Fig. 6J and K). This confirmed the previous result and showed that *drpr* expression in cortex glia is necessary for dead cell clearance in the MLpL region. However, dead cells were normally cleared in the lamina region in *wrapper* > *drpr*-RNAi, suggesting that lamina proximal glia is not essential for clearance (Fig. 6J). As discussed previously, it is suggested that another lamina cortex glia work for dead cell clearance together (redundantly) with distal lamina cortex glia. Then, lamina proximal cortex glia probably works for dead cell clearance.

Next, we investigated the time window of *drpr* expression required for dead cell clearance. *drpr*-RNAi was induced by shifting temperature from 25 °C to 30 °C at 48 h BPF (second larval instar) in *tub-Gal80*^{ts}; *wrapper-GAL4*>*drpr*-RNAi, dead cell clearance was suppressed. In contrast, when temperature shift was performed at 24 h BPF (early third instar), dead cells clearance was a little delayed, and when temperature was shifted at 12 h BPF (late third instar) or later stages dead cells were cleared normally (Fig. 6I, J and 6K). This suggests that expression of *drpr* from the second instar to early third instar is required for dead cell clearance. In previous experiment, heat shock at L3 and 0 h APF in hs-*GAL4*>*drpr*-RNAi insects suppressed dead cell clearance, but heat shock at 12 h APF or later stages did not, suggesting that *drpr* expression at late larval and early pupal stages is required for dead cell clearance (Fig. 2C). Altogether, we conclude *drpr* expression from second larval to early pupal stages is required for dead cell clearance. The reason for the inconsistency in results at late larval and early pupal stages between *tub-Gal80*^{ts}; *wrapper-GAL4*>*drpr*-RNAi and *hs-GAL4*>drpr-RNAi would be the difference in the strength of *drpr*-RNAi expression between them. That is, temporary expression of *drpr*-RNAi in *hs-GAL4*>*drpr*-RNAi would be stronger than *tub-Gal80*^{ts}; *wrapper*-GAL4>*drpr*-RNAi.

2.6. Role of Shark, dCed-6, Crk/Mbc/dCed-12, and Rac1 in clearance of dead neurons in the developing optic lobe

Next, we analyzed the function of known signaling molecules downstream of Drpr in the developing optic lobe. Shark and dCed-6 bind to Drpr and activate Rac1 downstream of Drpr (Fig. 7A) (Ziegenfuss et al., 2012). Crk, Mbc, and dCed-12 form a complex and activate Rac1 independently or downstream of Drpr. Previous studies reported that Shark, dCed-6, Crk/Mbc/dCed-12, and Rac1 in ensheathing glia in the adult olfactory lobe function to mediate removal of degenerating axons when the olfactory nerve is cut (Ziegenfuss et al., 2012), in astrocyte-like glia around the mushroom body when γ neuron axons are pruned (Awasaki et al., 2006; Tasdemir-Yilmaz and Freeman, 2014), and in astrocyte-like glia in the ventral nerve cord when vCrz neurons die during metamorphosis (Tasdemir-Yilmaz and Freeman, 2014). In contrast, Etchegaray et al. (2016) reported that these signaling molecules did not function to remove dead neurons in the brain. Here, we performed glial-specific knockdown of these molecules and examined whether dead neurons were cleared in the developing optic lobe.

The results showed that numerous TUNEL-positive cells accumulated in *repo* > *shark*-RNAi at 24 and 48 h APF (Fig. 7B and C). Therefore, Shark mediates clearance of dead neurons in the developing optic lobe. Moreover, in *repo* > *dced6*-RNAi (Awasaki et al., 2006), *crk*-RNAi (Tasdemir-Yilmaz and Freeman, 2014), *mbc*-RNAi (Tasdemir-Yilmaz and Freeman, 2014), *dced12*-RNAi (Lu et al., 2014), and *rac1*-RNAi (Ziegenfuss et al., 2012), a moderate effect was observed. About 1.5–4.2 times more dead cells than in the wild type accumulated at both 24 and 48 h APF (Fig. 7B and C) and clearance was delayed. This suggests that signaling molecules, dCed-6 and Crk/Mbc/dCed-12, partially mediate clearance of dead young neurons in the developing optic lobe and enhance it, but the role is minor. As cortex glia function to clear dead neurons via Drpr in the developing optic lobe, these signaling molecules must work in cortex glia in the developing optic lobe.

The Eiger/JNK pathway, which is activated by Drpr in ensheathing

glia and astrocyte-like glia, plays a role in efficient clearance of apoptotic neurons in the whole brain during metamorphosis (Hilu-Dadia et al., 2018). However, the present study suggested that the pathway plays no role in regulating clearance of cell bodies of dead neurons in the developing optic lobe (Fig. 7D and E).

2.7. Role of Pretaporter, CaBP1 and phosphatidylserine in clearance of dead neurons in the developing optic lobe

Next, we explored Drpr ligands in dead neurons in the developing optic lobe. Pretaporter (Prtp) and CaBP1 act as Drpr ligands when dead embryonic cells are phagocytosed by cultured cells in *Drosophila* (Kuraishi et al., 2009; Okada et al., 2012; Tung et al., 2013). However, no studies have investigated phagocytic ligands in the CNS in vivo. Therefore, we studied the function of these candidates for dead cell clearance in the developing optic lobe in Pretaporter and CaBP1 mutants.

The results showed a significant increase in the number of TUNEL-positive cells (about 2.2–2.6 times higher on average) at 48 h APF in $Prtp^{\Delta 1}$, $CaBP1^{\Delta 1}$, or $Prtp^{\Delta 1}$; $CaBP1^{\Delta 1}$ mutants compared to the wild type and clearance was delayed (Fig. 8A and B). Therefore, it was suggested that Pretaporter and CaBP1 acts as Drpr ligands and partially mediate dead cell clearance in the developing optic lobe. However, they are not essential and the role is minor.

Tung et al. (2013) showed that phosphatidylserine (PS), which acts as an "eat me" signal in the phagocytosis of apoptotic cells in mammals and nematodes, also serves as an "eat me" signal in the phagocytic removal of apoptotic cells in *Drosophila* and that Drpr is a PS-binding receptor for phagocytosis. Here, we tested whether phosphatidylserine also functions as a ligand for Drpr in clearance of dead neurons in the developing optic lobe. According to Tung et al. (2013), milk fat globule-epidermal growth factor 8 (MFG-E8) is a PS-binding protein of mammals, and when forcibly expressed, it binds to phosphatidylserine on dead cells via the C2 site and disrupts phagocytosis of dead cells in *Drosophila* embryos. When MFG-E8 was forcibly expressed with *repo-GAL4* or *actin-GAL4* in the developing Drosophila optic lobe, a significant increase in the number of TUNEL-positive cells (about 1.6 times higher on average) was observed at 24 h APF in comparison to the wild type (Fig. 8C, F). *elav* > MFG-E8 showed no increase in the number of TUNEL-positive cells. In contrast, forced expression of MFG-E8ΔC2, which lacks the phosphatidylserine binding C2 site, with any GAL4s did not affect the number of TUNEL-positive cells (Fig. 8D, F). These results support the idea of Tung et al. (2013) that phosphatidylserine mediates signaling for dead cell clearance.

Phosphatidylserine binds to Drpr via the EN site in its extracellular domain and induces phagocytosis (Tung et al., 2013). When we conducted forced expression of Drpr lacking the EN site (*drprΔEN*) on the *drpr* mutant background in *repo* > *drprΔEN;* $drpr^{\Delta 5}$, dead cell clearance was not rescued (Fig. 8E and F). Likewise, rescue was not observed in *elav* > *drprΔEN*; $drpr^{\Delta 5}$. This result supports the above idea and suggests a possibility that phosphatidylserine acts as a Drpr ligand and mediates dead cell clearance in the developing optic lobe.

Moreover, mutation in βInt-*ν*, which is another engulfment receptor in the embryo (Nonaka et al., 2013), significantly increased the number of TUNEL-positive cells at 24 h APF, but not at 48 h APF (Fig. 8G).

SIMU, which is another engulfment receptor in the embryonic CNS (Kurant et al., 2008) but not in the whole brain during metamorphosis (Etchegaray et al., 2016), played no role in clearance of dead neurons in the developing optic lobe (Fig. 8H).

3. Discussion

3.1. Cortex glia function to clear dead young neurons via the Drpr pathway in the developing optic lobe

In this study, we revealed that Drpr expressed in cortex glia were required for dead cell clearance in the MLpL region of the developing optic lobe, and that Drpr in other subtypes of glia did not mediate clearance. This is the first study that showed clearance of dead young neurons in the developing optic lobe required Drpr expression in the cortex glia. In the lamina region, lamina distal cortex glia work for dead cell clearance.

The expression pattern of Drpr agreed with the alteration in the activity of dead cell clearance in the optic lobe during metamorphosis. At early pupal stages, Drpr is expressed weakly in a mesh-like pattern and strongly in a centripetal pattern in cortex glia in the MLpL region. This expression weakened thereafter, and only weak expression was seen in a mesh-like pattern during the last half of the pupal period. Moreover, we observed no protrusion of Drpr expressing glial cytoplasm into the neuropil from neuropil glia (NG) at early pupal stages. This agrees with the fact that cell death in the developing optic lobe occurs mainly in young neurons before they extend neurites or in abnormal neurons with no neurites (Hara et al., 2018).

After 48 h APF, cell death was rarely observed and thus activity of dead cell clearance was low. However, this does not mean that glia lost potential ability to clear corpses at late pupal stages. Forced expression of wild-type *drpr* on the *drpr* mutant background at 48 or 72 h APF resulted in clearance of accumulated TUNEL-positive cells. This indicates that the components of the mechanism for dead cell clearance except Drpr are retained until late pupal stages. Therefore, if some cells died at late pupal stages and Drpr expression was induced in cortex glia, the dead cells would be cleared via Drpr pathway. Moreover, the fact that accumulated TUNEL-positive cells were removed when wild-type *drpr* was forcibly expressed in late pupal stages on the *drpr* mutant background suggests that "eat me" signals were secreted or displayed by accumulated TUNEL-positive cells in *drpr* mutants not only at early pupal stages, when the cells died, but also at late pupal stages long after cell death.

At late pupal stages, strong Drpr expression appeared in the cytoplasmic protrusions from the neuropil glia (NG), and astrocyte-like glia simultaneously started expressing molecular markers (specific GAL4s). This Drpr was not utilized for clearance of dead neurons, as almost no cell death arises at this stage in control conditions. In the neuropil of the optic lobe at late pupal stages, neurites extend and form synapses to make and complete neural networks (Fischbach and Hiesinger, 2008). When new synapses are formed during development of the *Drosophila* larval neuromuscular junction, significant amounts of presynaptic membranes and a subset of immature synapses are removed from the junction by surrounding glia and postsynaptic muscle via the Drpr/dCed-6 pathway (Fuentes-Medel et al., 2009). Thus, the same process may arise at developing synapses in the developing optic lobe, and astrocyte-like glia expressing Drpr in the cytoplasmic protrusions may function to remove unnecessary presynaptic membranes and immature synapses.

3.2. Role-sharing among glial subtypes in corpse clearance in the CNS

Previous studies have reported that astrocyte-like glia are responsible for clearance of degenerating axons of dying obsolete larval neurons in the ventral nerve cord (Tasdemir-Yilmaz and Freeman, 2014) and of pruned axons of γ neurons in the mushroom body (Awasaki and Ito, 2004; Tasdemir-Yilmaz and Freeman, 2014). In contrast, degenerating axons are removed by ensheathing glia in the olfactory lobe following Wallerian degeneration of the olfactory nerve (MacDonald et al., 2006; Doherty et al., 2009). Therefore, different subtypes of glia work to clear degenerating axons in different contexts. Astrocyte-like glia may specifically function for clearance of "programmed" degenerating axons and ensheathing glia for clearance of "accidently" degenerating axons. In addition, another subtype of glia, cortex glia, functions to remove dead young neurons. These young neurons had just started to differentiate into adult neurons in the developing optic lobe (Bertet et al., 2014; Erclik et al., 2017; Hara et al., 2018) and have not yet extended neurites at the time they die (Hara et al., 2018). Tasdemir-Yilmaz and Freeman (2014) reported that elimination of cell bodies of obsolete vCrz neurons requires Drpr, but its expression is not required in astrocyte-like glia. Young

neurons in the optic lobe and cell bodies of obsolete vCrz neurons in the ventral nerve cord both locate in the cortex and almost the same cellular materials are cleared after the cell death, including nucleus and general cytoplasm, but not neurites. Therefore, as with dead young neurons in the optic lobe, the expression of Drpr in cortex glia would be required for clearance of cell bodies of dead vCrz neurons. Comparative studies are expected in the future on the mechanisms for clearance of degenerating axons of dead neurons, degenerating axons of cut nerves, dead young neurons, and cell bodies of dead obsolete neurons. Moreover, considering that "accidently" degenerating axons are cleared by a different subtype of glia from "programmed" degenerating axons, a possibility should be tested that cell bodies of neurons that died "accidently" are cleared by a distinct subtype of glia.

3.3. Drpr/Shark/dCed-6 and Crk/Mbc/dCed-12 pathways are involved in clearance of dead young neurons in the developing optic lobe

This is the first study to reveal that Shark mediates Drpr-dependent clearance of dead neurons in the CNS. Moreover, this study suggests that Ced-6, Crk/Mbc/dCed-12, and Rac1 are partially involved in clearance of dead young neurons. Therefore, both Drpr/Shark/dCed-6 and Crk/Mbc/dCed-12 pathways work for dead cell clearance in the developing optic lobe. As cortex glia function for clearance of dead neurons in the developing optic lobe, these pathways must work in cortex glia.

A previous study reported that these pathways function to mediate removal of degenerating axons in ensheathing glia in the adult olfactory lobe when the olfactory nerve is cut (Ziegenfuss et al., 2012). The same pathways work in astrocyte-like glia around the mushroom body when axons of γ neurons are pruned (Awasaki and Ito, 2004; Tasdemir-Yilmaz and Freeman, 2014), and in the ventral nerve cord when neurites of dead vCrz neurons are cleared during metamorphosis (Tasdemir-Yilmaz and Freeman, 2014). Therefore, Drpr/Shark/dCed-6 and Crk/Mbc/dCed-12 pathways generally function to clear corpses in different glia in different contexts. However, the relative role played by each pathway depends on the situation. Although *drpr* mutation strikingly inhibited dead cell clearance in the optic lobe, knockdown of the Crk/Mbc/dCed-12 pathway had only a moderate effect. In contrast, removal of olfactory nerve axons that have undergone Wallerian degeneration is strongly affected by both *drpr* mutation and Crk/Mbc/dCed-12 knockdown (Ziegenfuss et al., 2012). In the pruning of mushroom body γ axons, mutation of *drpr* and knockdown of Crk/Mbc/dCed-12 additively affect clearance, although mutation of *drpr* has a stronger effect (Tasdemir-Yilmaz and Freeman, 2014). In the removal of axons from dead vCrz neurons during metamorphosis, knockdown of *dCed-12* causes a moderate defect, whereas *drpr* mutation causes no defect by itself but only enhances the defect caused by *dCed-12* knockdown (Tasdemir-Yilmaz and Freeman, 2014). How the relative role of these pathways is regulated and why remain to be defined.

3.4. Role of candidate ligands for Drpr, Pretaporter, CaBP1 and phosphatidylserine, in dead cell clearance in the developing optic lobe

Previous studies reported that Pretaporter, CaBP1 and phosphatidylserine act as Drpr ligands when dead embryonic cells are phagocytosed in the *Drosophila* embryo and cultured cells (Kuraishi et al., 2009; Okada et al., 2012; Tung et al., 2013). The present study suggested a possibility that these molecules mediate signaling for dead cell clearance as a Drpr ligand in the developing optic lobe. However, Pretaporter and CaBP1 are not essential for clearance and their role would be minor. Therefore, relative role of molecules that work for dead cell clearance as ligands for Drpr may be different depending on the context. As described above, different subtypes of glia work to clear corpse in the CNS: ensheathing glia for Wallerian's degenerating axons, astrocyto-like glia for pruned axons and degenerating axons of dead vCrz neurons, and cortex glia for dead young neurons in the optic lobe. Therefore, it is to be defined whether difference in ligand molecules is involved in activating different subtypes of glia.

3.5. Possible causes for inconsistencies between the present study and previous ones

The present study agrees with results described by Tasdemir-Yilmaz and Freeman (2014), who reported that Drpr is required for elimination of cell bodies of vCrz neurons that die at 3–7 h APF (Lee et al., 2011). However, the current study disagrees with other studies (Etchegaray et al., 2016; Hilu-Dadia et al., 2018).

Several possible causes may have led to these inconsistencies. One possibility is the difference in cellular materials to be cleared, that is, cell bodies or neurites, as mentioned earlier. The present study examined dead young neurons in the developing optic lobes. Cellular materials to be cleared include only nucleus and general cytoplasm, but not neurites (Hara et al., 2018). Tasdemir-Yilmaz and Freeman (2014) studied vCrz neurons and found that molecular mechanisms for clearance of cell bodies and neurites are different. However, other studies examined the central brain or the whole brain, which include cell bodies of dead neurons, neurites of dead neurons and pruned neurites. Another possibility is the difference in methods to detect dead neurons. We used the ABC TUNEL method, which detects degraded DNA in dead cell nuclei with the streptavidin-biotin-peroxidase complex (Vector Laboratories). This method is far more sensitive and reliable than the fluorescent TUNEL method (compare the number of TUNEL-positive cells between the present study and other studies). Another method to detect dead cells is anti-Dcp-1 antibody staining. This method has some problems with detection of accumulated dead cell corpses in phagocytosis-defective mutants. It detects activated Dcp-1, one of the effector caspases (Cell Signaling Technology, Data Sheet). However, another effector caspase, DrIce (Akagawa et al., 2015), is also expressed and is a more effective inducer of apoptosis than Dcp-1 (Florentin and Arama, 2012). Therefore, this method may not detect all dead cells. Another problem with this method is the unknown stability of activated Dcp-1 in dead cells. Therefore, detection of activated Dcp-1 does not show exactly how many dead cells have accumulated in phagocytosis-defective mutants. Moreover, when dendrites are pruned during remodeling of dendritic arborization sensory neurons during metamorphosis, caspase activity is detected in the dendrite (Williams et al., 2006). This suggests that the anti-Dcp-1 antibody may detect pruned dendrites as well as dead cells. Finally, the subtypes of glia that clear corpses are also different in the present study and previous ones. We found that expression of GAL4 in glia subtype-specific GAL4 lines drastically changed during metamorphosis, and the expression pattern at pupal stages was different from adult stages in many GAL4 lines. However, previous studies did not examine the expression pattern of the GAL4 lines they used. Altogether, studies on a single type of dead neuron or identified neurons are required in the future. The mechanisms for clearance of dead cell bodies and degenerating neurites should be studied independently. The expression pattern of GAL4 lines in subtypes of glia should be carefully assessed before using the line as a GAL4 driver.

4. Materials and methods

4.1. Fly strains

Canton-Special was used as the wild-type strain. We used nine GAL4 lines for tissue/time-specific RNAi or forced expression: *hs-GAL4* (Halfon et al., 1997), *M1B repo-GAL4* (Sepp et al., 2001), *C155 elav-GAL4* (Lin and Goodman, 1994), *crq-GAL4* (Olofsson and Page, 2005), NP6099 (DGRC #105125) (Hayashi et al., 2002), *esg-GAL4* (DGRC #104863) (Hayashi et al., 2002), *tub-GAL80^{ts}* (McGuire et al., 2003), *wrapper* (GMR54H02)-*GAL4* (DGRC #45784) and *actin-GAL4* (Ito et al., 1997). We used eight GAL4 lines for analysis of glial subtypes: *NP0577* (DGRC #112228), *NP1243* (*wun^{NP1243}*, DGRC #103953), *NP2222* (*Akap200^{NP2222}*, DGRC #112830), *NP2276* (*spin^{NP2276}*, DGRC #112853),

NP3233 (DGRC #113173), *NP6293* (*Bsg*^{NP6293}, DGRC #105188), *NP6520* (DGRC #105240) (Hayashi et al., 2002), and *alrm-GAL4* (Doherty et al., 2009). We used 14 UAS lines: *UAS-draper-RNAi* (VDRC #27086), *UAS-draper1* (McPhee et al., 2010), *UAS-mCD8::GFP* (Lee and Luo, 1999), *UAS-shark-RNAi* (VDRC #105706), *UAS-ced6-RNAi* (NIG #11804-R1; Awasaki et al., 2006), *UAS-crk-RNAi* (VDRC #19061; Tasdemir-Yilmaz and Freeman, 2014), *UAS-mbc-RNAi* (VDRC #16044; Tasdemir-Yilmaz and Freeman, 2014), *UAS-dced12-RNAi* (VDRC #10455; Lu et al., 2014), *UAS-rac1-RNAi* (VDRC #49246; Ziegenfuss et al., 2012), *UAS-MFG-E8*, *UAS-MFG-E8ΔC2*, *UAS-draperΔEN* (Tung et al., 2013), *UAS-SIMU-RNAi* (VDRC #101915), and *UAS-bsk*^{DN} (Adachi-Yamada et al., 1999). We used seven mutants: *draper*$^{\Delta 5}$ (Freeman et al., 2003), *Pretaporter*$^{\Delta 1}$ (Kuraishi et al., 2009), *CaBP1*$^{\Delta 1}$ (Okada et al., 2012), β-Int ν1, β-Int ν2 (Devenport and Brown, 2004), *SIMU*^{KO} (Kurant et al., 2008), and *eiger*$^{[3]}$ (Igaki et al., 2002). Flies were reared on a general cornmeal-yeast medium at 25 °C under a 12-h/12-h light/dark photoperiod.

4.2. Detection of dying cells

A modified version of the TUNEL method described by Kimura (1995) was used to detect dying cells. Briefly, brains were excised, washed in phosphate-buffered saline (PBS), fixed in 4% formaldehyde, washed with 0.3% Triton-X 100 in PBS (v/v) (PBT), and stored in methanol at −20 °C for at least one night. These brains were then washed with PBT, treated with 10 μg/ml Protease K (Wako Pure Chemical Industries, Osaka) for 10 min at room temperature, and fixed again in 4% formaldehyde. The brains were subsequently washed with PBT, pretreated in terminal deoxynucleotidyl transferase (TdT) buffer, and incubated overnight at 37 °C in TdT reaction solution (Takara Bio, Shiga) with biotin-16-dUTP (Roche Diagnostics, Mannheim). The brains were next washed with PBT and incubated in ABC reaction solution (Vector Laboratories, Burlingame) for 1 h at room temperature. After washing with PBT, the brains were stained using a standard brown horseradish peroxidase reaction with 3,3′-diaminobenzidine (0.01%) and hydrogen peroxide (0.001%). Dying cells appeared dark brown in about 45 min. After the reaction, the brains were washed with distilled water, dehydrated in a series of ethanol solutions of increasing concentrations, cleared with methyl benzoate, and embedded in Canada Balsam:methyl benzoate 3:1 (V:V) on a glass slide. The specimens were inspected with bright-field microscopy (Optiphot, Nikon, Tokyo).

4.3. Analysis of the number and distribution of dying cells

We used a light microscope, a × 40 objective lens, and a digital camera (TS-CA series, Sugitoh, Tokyo) to acquire images of dying cells; we then digitally enlarged these images to × 1000 on a monitor. We used images from the anterior view to count the number of dying cells. While we gradually shifted the focus manually, each signal larger than 0.7 μm in diameter was scored as a TUNEL-positive cell with a dot on a transparent plastic sheet that was affixed to the monitor. The images were captured digitally with a scanner, and the number of dots was counted using the particle counter module of the NIH ImageJ software package. For analysis of the spatial distribution of dying cells, we obtained images of 1 μm-thick serial optical sections that were taken from a dorsal view. An optical microscope (BX50, Olympus, Tokyo), a digital camera (DP72, Olympus), and Metamorph software (MDS Analytical Technologies, Sunnyvale) were used for this imaging.

Statistical analysis was performed using "R". Variance was analyzed using the Kruskal-Wallis rank sum test, and post hoc pairwise comparisons were performed using the Wilcoxon rank sum test with Bonferroni correction and the Mann-Whitney test. In *drpr* mutants and *drpr*-RNAi samples, TUNEL-positive signals overlapped at the periphery of the optic lobe in almost all samples of the group, and we could not count the exact number of TUNEL-positive cells (Fig. 1A and B). Therefore, we described the number of TUNEL-positive cells in optic lobes of such groups as "uncountable" in this study, and statistical analysis was performed among groups other than these.

4.4. Heat induction of drpr-RNAi and wild-type Drpr

To induce *drpr*-RNAi on the wild-type background or to induce wild-type *drpr1* in *drpr*$^{\Delta 5}$ mutants before puparium formation, late third instar larvae were placed into 1.5-ml microcentrifuge tubes, and the tubes were incubated for 30 min in a 37 °C water bath. Then, the larvae were transferred into new culture vials and maintained at 25 °C. Larvae that underwent puparium formation 12–16 h after this heat shock were used for the experiments. To induce *drpr*-RNAi on the wild-type background or to induce *draper1* in *drpr*$^{\Delta 5}$ mutants after puparium formation, pupae at 0, 12, 24, 48, and 72 h APF were placed into 1.5-ml microcentrifuge tubes, and the tubes were incubated for 1 h in a 37 °C water bath. Then the pupae were reared at 25 °C and used for the experiment at the appropriate stage. The reason why we heat-shocked only for 0.5 h for late third instar larvae is that heat shock for 1 h at this stage killed all the larvae.

4.5. Induction of drpr-RNAi by temperature shift using GAL80^{ts}

Time window of *drpr* expression required for dead cell clearance was determined using GAL80^{ts}; *wrapper-GAL4*>drpr-RNAi insects. For temperature shift at 12 h, 24 h and 48 h BPF, culture vials with growing larvae or pupae were moved from 25 °C into a 30 °C water bath, and insects that formed puparium 12 h, 24 h and 48 h after temperature shift were picked up and placed into a new culture vial at 30 °C. For temperature shift at 0 h and 24 h APF, pupae just after puparium formation were picked up and placed into a new culture vial at 30 °C. Then, pupae were maintained at 30 °C to 48 h APF and dissected.

4.6. Immunohistochemistry and confocal microscopy

Pupal brains were dissected from whole animals in PBS and fixed in 4% formaldehyde for 20 min. These samples were then washed with PBT and incubated in PBT containing a blocking agent (5% normal goat serum) for 30 min. Samples were then incubated in PBT containing one or two of the following primary antibodies. The primary antibodies were used at the following dilutions: anti-Draper (Draper 5D14-s, DSHB) (1:20), anti-N-cadherin (DN-EX #8-s, DSHB, Iwai et al., 1997) (1:20), and anti-Repo (8D12 anti-Repo, DSHB, Alfonso and Jones, 2002) (1:20), anti-Croquemort (Manaka et al., 2004) (1:1000). Samples were washed in PBT for 1 h and then incubated in PBT containing 5% normal goat serum for 30 min and finally in PBT containing secondary antibodies. The following secondary antibodies were used: anti-mouse IgG Texas Red (ROCKLAND, Gilbertsville) (1:500), anti-mouse IgG Cy5 (Abcam, Cambridge) (1:100), anti-rat IgG FITC (KPL, Guildford) (1:100), and anti-rat IgG Cy5 (Biological Detection Systems, Pittsburgh) (1:100). After washing for 1 h with PBT, the antibody-labeled samples were processed with 50% glycerol (for fluorescence microscopy, MERCK, Darmstadt) and mounted with 80% glycerol. All images were obtained with a LSM 710 microscope (Carl Zeiss, Oberkochen) and TSC-SP5 (Leica Microsystems, Wetzlar); the images were processed with Zen2009 light edition (Carl Zeiss), Las AF (Leica Microsystems), and Photoshop (Adobe, San Jose).

4.7. Lysotracker staining

Brains were excised, washed in PBS, treated with 0.02% Lysotracker in PBS (v/v) (Lysotracker Red DND-99, Invitrogen/Molecular Probes, Tokyo) for 30 min, washed with PBS, fixed in 4% formaldehyde for 20 min, and washed with PBT for 30 min. The samples were then incubated for 30 min in PBT containing a blocking agent (5% normal goat serum) and then incubated overnight at 4 °C in PBT containing the primary antibodies anti-Repo (8D12 anti-Repo, DSHB, Alfonso and Jones,

2002) (1:20) and anti-N-cadherin (DN-EX #8-s, DSHB, Iwai et al., 1997) (1:20). Samples were washed in PBT for 1 h, incubated in PBT containing 5% normal goat serum for 30 min, and then incubated in PBT containing secondary antibodies overnight at 25 °C. The secondary antibodies were anti-mouse IgG Texas Red (ROCKLAND) (1:100) and anti-rat IgG Cy5 (Biological Detection Systems) (1:100). After washing for 1 h, the antibody-labeled samples were mounted in 80% glycerol (for fluorescence microscopy, MERCK).

Conflicts of interest

The authors declare no competing or financial interests.

Author contributions

RN, MI and HT conceived, designed and analyzed the experiments. RN, MI, AO, YT and YH performed most experiments. TF, MT and TTS officially supervised RN and AO after the retirement of HT. RN and HT wrote the manuscript.

Funding

This research did not receive any specific grant from funding agencies in the public, commercial, or not-for-profit sectors.

Acknowledgments

We thank the *Drosophila* Genetic Resource Center at Kyoto Institute of Technology, the Bloomington *Drosophila* Stock Center at Indiana University, Vienna *Drosophila* Resource Center at the Vienna Biocenter, Dr. M.R. Freeman at the University of Massachusetts Medical School, Dr. Y. Nakanishi at Kanazawa University, and Dr. T. Awasaki at Kyorin University for providing fly stocks. We thank the Developmental Studies Hybridoma Bank at the University of Iowa, and Dr. Y. Nakanishi at Kanazawa University for providing antibodies. We thank Dr. T. Igaki at Kyoto University for allowing R. Nakano to complete this project in his laboratory.

References

Adachi-Yamada, T., Nakamura, M., Irie, K., Tomoyasu, Y., Sano, Y., Mori, E., Goto, S., Ueno, N., Nishida, Y., Matsumoto, K., 1999. p38 mitogen-activated protein kinase can be involved in transforming growth factor beta superfamily signal transduction in *Drosophila* wing morphogenesis. Mol. Cell Biol. 19 (3), 2322–2329.

Akagawa, H., Hara, Y., Togane, Y., Iwabuchi, K., Hiraoka, T., Tsujimura, H., 2015. The role of the effector caspase *drICE* and *dcp-1* for cell death and corpse clearance in the developing optic lobe in *Drosophila*. Dev. Biol. 404 (2), 61–75.

Alfonso, T.B., Jones, B.W., 2002. gcm2 promotes glial cell differentiation and is required with glial cells missing for macrophage development in *Drosophila*. Dev. Biol. 248 (2), 369–383.

Awasaki, T., Ito, K., 2004. Engulfing action of glial cells is required for programmed axon pruning during *Drosophila* metamorphosis. Curr. Biol. 14 (8), 668–677.

Awasaki, T., Tatsumi, R., Takahashi, K., Arai, K., Nakanishi, Y., Ueda, R., Ito, K., 2006. Essential role of the apoptotic cell engulfment genes draper and ced-6 in programmed axon pruning during *Drosophila* metamorphosis. Neuron 50 (6), 855–867.

Awasaki, T., Lai, S.L., Ito, K., Lee, T., 2008. Organization and postembryonic development of glial cells in the adult central brain of *Drosophila*. J. Neurosci. 28 (51), 13742–13752.

Bertet, C., Li, X., Erclik, T., Cavey, M., Wells, B., Desplan, C., 2014. Temporal patterning of neuroblasts controls notch-mediated cell survival through regulation of hid or reaper. Cell 158 (5), 1173–1186.

Cantera, R., Technau, G.M., 1996. Glial cells phagocytose neuronal debris during the metamorphosis of the central nervous system in *Drosophila melanogaster*. Dev. Gene. Evol. 206 (4), 277–280.

Chen, Z., Rodriguez, A.D.V., Li, X., Erclik, T., Fernandes, V.M., Desplan, C., 2016. A unique class of neural progenitors in the Drosophila optic lobe generates both migrating neurons and glia. Cell Rep. 15, 774–786.

Choi, Y.J., Lee, G., Park, J.H., 2006. Programmed cell death mechanisms of identifiable peptidergic neurons in *Drosophila melanogaster*. Development 133 (11), 2223–2232.

Consoulas, C., Restifo, L.L., Levine, R.B., 2002. Dendritic remodeling and growth of motoneurons during metamorphosis of *Drosophila melanogaster*. J. Neurosci. 22 (12), 4906–4917.

Devenport, D., Brown, N.H., 2004. Morphogenesis in the absence of integrins: mutation of both *Drosophila* beta subunits prevents midgut migration. Development 131 (21), 5405–5415.

Doherty, J., Logan, M.A., Tasdemir, O.E., Freeman, M.R., 2009. Ensheathing glia function as phagocytes in the adult *Drosophila* brain. J. Neurosci. 29 (15), 4768–4781.

Edwards, T.N., Meinertzhagen, I.A., 2010. The functional organization of glia in the adult brain of *Drosophila* and other insects. Prog. Neurobiol. 90 (4), 471–497.

Edwards, T.N., Nuschke, A.C., Nern, A., Meinertzhagen, I.A., 2012. Organization and metamorphosis of glia in the *Drosophila* visual system. J. Comp. Neurol. 520 (1), 2067–2085.

Erclik, T., Li, X., Courgeon, M., Bertet, C., Chen, Z., Baumert, R., Ng, J., Koo, C., Arain, U., Behnia, R., del Valle Rodriguez, A., Senderowicz, L., Negre, N., White, K.P., Desplan, C., 2017. Integration of temporal and spatial patterning generates neural diversity. Nature 541 (7637), 365–370.

Etchegaray, J.I., Elguero, E.J., Tran, J.A., Sinatra, V., Feany, M.B., McCall, K., 2016. Defective phagocytic corpse processing results in neurodegeneration and can be rescued by TORC1 activation. J. Neurosci. 36 (11), 3170–3183.

Fischbach, K.F., Technau, G., 1984. Cell degeneration in the developing optic lobes of the sine oculis and small-optic-lobes mutants of *Drosophila melanogaster*. Dev. Biol. 104 (1), 219–239.

Fischbach, K.F., Hiesinger, P.R., 2008. Optic lobe development. In: Brain Development in Drosophila melanogaster, vol. 628, pp. 115–136. Adv. Exp. Med. Biol.

Florentin, A., Arama, E., 2012. Caspase levels and execution efficiencies determine the apoptotic potential of the cell. J. Cell Biol. 196 (4), 513–527.

Freeman, M.R., Delrow, J., Kim, J., Johnson, E., Doe, C.Q., 2003. Unwrapping glial biology: gcm target genes regulating glial development, diversification, and function. Neuron 38 (4), 567–580.

Fuentes-Medel, Y., Logan, M.A., Ashley, J., Ataman, B., Budnik, V., Freeman, M.R., 2009. Glia and muscle sculpt neuromuscular arbors by engulfing destabilized synaptic boutons and shed presynaptic debris. PLoS Biol. 7 (8), e1000184.

Halfon, M.S., Kose, H., Chiba, A., Keshishian, H., 1997. Targeted gene expression without a tissue-specific promoter: creating mosaic embryos using laser-induced single-cell heat shock. Proc. Natl. Acad. Sci. U.S.A. 94 (12), 6255–6260.

Hara, Y., Hirai, K., Togane, Y., Akagawa, H., Iwabuchi, K., Tsujimura, H., 2013. Ecdysone-dependent and ecdysone-independent programmed cell death in the developing optic lobe of *Drosophila*. Dev. Biol. 374 (1), 127–141.

Hara, Y., Sudo, T., Togane, Y., Akagawa, H., Tsujimura, H., 2018. Cell death in neural precursor cells and neurons before neurite formation prevents the emergence of abnormal neural structures in the *Drosophila* optic lobe. Dev. Biol. 436 (1), 28–41.

Hayashi, S., Ito, K., Sado, Y., Taniguchi, M., Akimoto, A., Takeuchi, H., Aigaki, T., Matsuzaki, F., Nakagoshi, H., Tanimura, T., Ueda, R., Uemura, T., Yoshihara, M., Goto, S., 2002. GETDB, a database compiling expression patterns and molecular locations of a collection of Gal4 enhancer traps. Genesis 34 (1–2), 58–61.

Hilu-Dadia, R., Hakim-Mishnaevski, K., Levy-Adam, F., Kurant, E., 2018. Draper-mediated JNK signaling is required for glial phagocytosis of apoptotic neurons during *Drosophila* metamorphosis. Glia 66 (7), 1520–1532.

Igaki, T., Kanda, H., Yamamoto-Goto, Y., Kanuka, H., Kuranaga, E., Aigaki, T., Miura, M., 2002. Eiger, a TNF superfamily ligand that triggers the *Drosophila* JNK pathway. EMBO J. 21 (12), 3009–3018.

Ito, K., Awano, W., Suzuki, K., Hiromi, Y., Yamamoto, D., 1997. The *Drosophila* mushroom body is a quadruple structure of clonal units each of which contains a virtually identical set of neurones and glial cells. Development 124 (4), 761–771.

Iwai, Y., Usui, T., Hirano, S., Steward, R., Takeichi, M., Uemura, T., 1997. Axon patterning requires *D*N-cadherin, a novel adhesion receptor, in the *Drosophila* embryonic CNS. Neuron 19 (1), 77–89.

Jiang, Y., Reichert, H., 2012. Programmed cell death in type II neuroblast lineages is required for cental complex development in the *Drosophila* brain. Neural Dev. 7, 3.

Kimura, K., 1995. Drosophila melanogaster. In: Tsujimoto, Y., Tone, S., Yamada, T. (Eds.), The Newest Experimental Methods for Apoptosis Research. Yodosha, Tokyo, Japan, pp. 227–235.

Kremer, M.C., Jung, C., Batelli, S., Rubin, G.M., Gaul, U., 2017. The glia of the adult *Drosophila* nervous system. Glia 65 (4), 608–638.

Kuraishi, T., Nakagawa, Y., Nagaosa, K., Hashimoto, Y., Ishimoto, T., Moki, T., Fujita, Y., Nakayama, H., Dohmae, N., Shiratsuchi, A., Yamamoto, N., Ueda, K., Yamaguchi, M., Awasaki, T., Nakanishi, Y., 2009. Pretaporter, a *Drosophila* protein serving as a ligand for Draper in the phagocytosis of apoptotic cells. EMBO J. 28 (24), 3868–3878.

Kurant, E., Axelrod, S., Leaman, D., Gaul, U., 2008. Six-microns-under acts upstream of Draper in the glial phagocytosis of apoptotic neurons. Cell 133 (3), 498–509.

Kurant, E., 2011. Keeping the CNS clear: glial phagocytic functions in *Drosophila*. Glia 59 (9), 1304–1311.

Lee, G., Wang, Z., Sehgal, R., Chen, C.H., Kikuno, K., Hay, B., Park, J.H., 2011. *Drosophila* caspases involved in developmentally regulated programmed cell death of peptidergic neurons during early metamorphosis. J. Comp. Neurol. 519 (1), 34–48.

Lee, T., Luo, L., 1999. Mosaic analysis with a repressible cell marker for studies of gene function in neuronal morphogenesis. Neuron 22 (3), 451–461.

Lin, D.M., Goodman, C.S., 1994. Ectopic and increased expression of Fasciclin II alters motoneuron growth cone guidance. Neuron 13 (3), 507–523.

Lu, T., Doherty, J., Freeman, M.R., 2014. DRK/DOS/SOS converge with Crk/Mbc/dCed-12 to activate Rac1 during glial engulfment of axonal debris. Proc. Natl. Acad. Sci. U.S.A. 111 (34), 12544–12549.

MacDonald, J.M., Beach, M.G., Porpiglia, E., Sheehan, A.E., Watts, R.J., Freeman, M.R., 2006. The *Drosophila* cell corpse engulfment receptor Draper mediates glial clearance of severed axons. Neuron 50 (6), 869–881.

Manaka, J., Kuraishi, T., Shiratsuchi, A., Nakai, Y., Higashida, H., Henson, P., Nakanishi, Y., 2004. Draper-mediated and phosphatidylserine-independent

phagocytosis of apoptotic cells by *Drosophila* hemocytes/macrophages. J. Biol. Chem. 279 (46), 48466–48476.
McGuire, S.E., Le, P.T., Osborn, A.J., Matsumoto, K., Davis, R.L., 2003. Spatiotemporal rescue of memory dysfunction in *Drosophila*. Science 302 (5651), 1765–1768.
McPhee, C.K., Logan, M.A., Freeman, M.R., Baehrecke, E.H., 2010. Activation of autophagy during cell death requires the engultment receptor Draper. Nature 465 (7301), 1093–1096.
Meinertzhagen, I.A., Hanson, T.E., 1993. The Development of the optic lobe. In: Bate, M., Arias, A.M. (Eds.), The Development of *Drosophila Melanogaster*. Cold Spring Harbor Laboratory Press, New York, pp. 1363–1491.
Nakano, Y., Fujitani, K., Kurihara, J., Ragan, J., Usui-Aoki, K., Shimoda, L., Lukacsovich, T., Suzuki, K., Sezaki, M., Sano, Y., Ueda, R., Awano, W., Kaneda, M., Umeda, M., Yamamoto, D., 2001. Mutations in the novel membrane protein spinster interfere with programmed cell death and cause neural degeneration in *Drosophila melanogaster*. Mol. Cell Biol. 21 (11), 3775–3788.
Nonaka, S., Nagaosa, K., Mori, T., Shiratsuchi, A., Nakanishi, Y., 2013. Integrin αPS3/βν-mediated phagocytosis of apoptotic cells and bacteria in *Drosophila*. J. Biol. Chem. 288 (15), 10347–10380.
Okada, R., Nagaosa, K., Kuraishi, T., Nakayama, H., Yamamoto, N., Nakagawa, Y., Dohmae, N., Shiratsuchi, A., Nakanishi, Y., 2012. Apoptosis-dependent externalization and involvement in apoptotic cell clearance of DmCaBP1, an endoplasmic reticulum protein of *Drosophila*. J. Biol. Chem. 287 (5), 3138–3146.
Robinow, S., Talbot, W.S., Hogness, D.S., Truman, J.W., 1993. Programmed cell death in the *Drosophila* CNS is ecdysone-regulated and coupled with a specific ecdysone receptor isoform. Development 119 (4), 1251–1259.
Sato, M., Suzuki, T., Nakai, Y., 2013. Waves of differentiation in the fly visual system. Dev. Biol. 380 (1), 1–11.
Sepp, K.J., Schulte, J., Auld, V.J., 2001. Peripheral glia direct axon guidance across the CNS/PNS transition zone. Dev. Biol. 238 (1), 47–63.
Sonnenfeld, M.J., Jacobs, J.R., 1955. Macrophages and glia participate in the removal of apoptotic neurons from the Drosophila embryonic nervous system. J. Comp. Neurol. 359, 644–652.
Tasdemir-Yilmaz, O.E., Freeman, M.R., 2014. Astrocytes engage unique molecular programs to engulf pruned neuronal debris from distinct subsets of neurons. Genes Dev. 28 (1), 20–33.
Togane, Y., 2012. Cell Death and Morphogenesis in the Drosophila Optic Lobe during Metamorphosis. Tokyo Univ. Agri. Tech.. Doctoral thesis.
Togane, Y., Ayukawa, R., Hara, Y., Akagawa, H., Iwabuchi, K., Tsujimura, H., 2012. Spatio-temporal pattern of programmed cell death in the developing *Drosophila* optic lobe. Dev. Growth Differ. 54 (4), 503–518.
Truman, J.W., Taylor, B.J., Awad, T.A., 1993. Formation of the adult nervous system. In: Bate, M. (Ed.), The Development of *Drosophila melanogaster*. Cold Spring Harbor Laboratory Press, pp. 1245–1275.
Tung, T.T., Nagaosa, K., Fujita, Y., Kita, A., Mori, H., Okada, R., Nonaka, S., Nakanishi, Y., 2013. Phosphatidylserine recognition and induction of apoptotic cell clearance by *Drosophila* engulfment receptor Draper. J. Biochem. 153 (5), 483–491.
Williams, D.W., Kondo, S., Krzyzanowska, A., Hiromi, Y., Truman, J.W., 2006. Local caspase activity directs engulfment of dendrites during pruning. Nat. Neurosci. 9 (10), 1234–1236.
Winbush, A., Weeks, J.C., 2011. Steroid-triggered, Cell-autonomous death of a *Drosophila* motoneuron during metamorphosis. Neural Dev. 6, 15.
Ziegenfuss, J.S., Doherty, J., Freeman, M.R., 2012. Distinct molecular pathways mediate glial activation and engulfment of axonal debris after axotomy. Nat. Neurosci. 15 (7), 979–987.